AUTOMATED HYBRID WATER HEATING SYSTEM

A Final Year Project Report

Presented to

SCHOOL OF MECHANICAL & MANUFACTURING ENGINEERING

Department of Mechanical Engineering

NUST

ISLAMABAD, PAKISTAN

In Partial Fulfillment

of the Requirements for the Degree of

Bachelor of Mechanical Engineering

by

Ahsan Munib Khalid

Fareed Ahmad Abdani

Bariq Iqbal Sandhu

June 2022

EXAMINATION COMMITTEE

We hereby recommend that the final year project report prepared under our supervision by:

Ahsan Munib Khalid	**250841**
Fareed Ahmad Abdani	**245970**
Bariq Iqbal Sandhu	**235290**

Titled: "AUTOMATED HYBRID WATER HEATING SYSTEM" be accepted in partial fulfillment of the requirements for the award of Mechanical Engineering degree with grade ___

Supervisor: Dr. Muhammad Usman Bhutta Dept. of Mechanical Engineering	Dated:
Committee Member: Name, Title (faculty rank) Affiliation	Dated:
Committee Member: Name, Title (faculty rank) Affiliation	Dated:

Dated: _____ _____

(Head of Department)

COUNTERSIGNED

Dated: _____ _____

(Dean / Principal)

CONTENTS

LIST OF FIGURES

LIST OF TABLES

ABSTRACT

The aim of this Project is to Develop a Fully Automated Hybrid Solar Water Heating System. The system would be based on the Hybrid PVT Panels. PVT panels produce dual output, as electrical energy as well as thermal heat. PVT panels thus generate a higher desirable output for the same covered area in comparison to conventional PV Panels and have been reported to have longer operational /service life. This project would utilize these panels to design and implement a fully automated system that would not only heat but also maintain the temperature at the desired level. The automation would be achieved by Instrumentation, Real-Time Data Acquisition, and implementation Feed-Back Control Algorithms. There is a large segment of society and industries such as Hospitals & Healthcare Services, University & School Campuses, Breweries & Distilleries, Food & Beverage Processing Plants, Commercial Laundry Facilities, Textile Manufacturing Facilities, Automotive OEMs, etc. which can benefit from this project.

Our proposed method not only addresses the issue of global warming but also focuses on the accuracy, functionality, scalability throughput, carbon footprint, resolution, and overall cost-effectiveness of the product by having a bespoke real-time feedback-controlled system that will bring economic benefit to a company.

ACKNOWLEDGMENTS

We would like to thank Allah Almighty for enabling us to successfully conduct this project. Secondly, we extend our heartfelt gratitude to our supervisor, Dr. Muhammad Usman Bhutta, whose able support, and guidance helped us during our project. Next, we thank all our instructors at SMME who imparted the requisite knowledge which helped us complete our project. Furthermore, we would like to thank Dr. Adeel Waqas and Sir Qamar from USPCASE for their assistance in the fabrication and testing of the project. Finally, we would like to thank our families, especially our parents, whose unconditional support and prayers motivated us during the Final Year Project.

ORIGANLITY REPORT

19%	13%	11%	10%
SIMILARITY INDEX	INTERNET SOURCES	PUBLICATIONS	STUDENT PAPERS

PRIMARY SOURCES

1	Oussama Rejeb, Mohammad Sardarabadi, Christophe Ménézo, Mohammad Passandideh-Fard, Mohamed Houcine Dhaou, Abdelmajid Jemni. "Numerical and model validation of uncovered nanofluid sheet and tube type photovoltaic thermal solar system", Energy Conversion and Management, 2016 Publication	3%
2	forum.arduino.cc Internet Source	3%
3	Submitted to University of Wolverhampton Student Paper	1%
4	Submitted to Riga Technical University Student Paper	1%
5	Submitted to Higher Education Commission Pakistan Student Paper	1%
6	www.mdpi.com Internet Source	1%

7	Rejeb, Oussama, Mohammad Sardarabadi, Christophe Ménézo, Mohammad Passandideh-Fard, Mohamed Houcine Dhaou, and Abdelmajid Jemni. "Numerical and model validation of uncovered nanofluid sheet and tube type photovoltaic thermal solar system", Energy Conversion and Management, 2016. Publication	1 %
8	Y. A. Sheikh, A. D. Butt, K. N. Paracha, A. B. Awan, A. R. Bhatti, M. Zubair. "An improved cooling system design to enhance energy efficiency of floating photovoltaic systems", Journal of Renewable and Sustainable Energy, 2020 Publication	<1 %
9	Submitted to De Montfort University Student Paper	<1 %
10	Submitted to Nelson Marlborough Institute of Technology Student Paper	<1 %
11	Submitted to Curtin University of Technology Student Paper	<1 %
12	www.maximintegrated.com Internet Source	<1 %
13	Submitted to American University in Cairo Student Paper	<1 %

14	create.arduino.cc Internet Source	<1 %
15	Jian Sun, Mingheng Shi. "Numerical Simulation of Electric-Thermal Performance of a Solar Concentrating Photovoltaic/Thermal System", 2009 Asia-Pacific Power and Energy Engineering Conference, 2009 Publication	<1 %
16	Submitted to University of Surrey Student Paper	<1 %
17	circuitdigest.com Internet Source	<1 %
18	Submitted to Engineers Australia Student Paper	<1 %
19	Submitted to American University of the Middle East Student Paper	<1 %
20	Submitted to TAFE SA Student Paper	<1 %
21	Submitted to Universiti Teknikal Malaysia Melaka Student Paper	<1 %
22	wiredspace.wits.ac.za Internet Source	<1 %
23	coek.info Internet Source	

		<1 %
24	pastebin.com Internet Source	<1 %
25	www.fupress.com Internet Source	<1 %
26	"Proceedings of International Conference in Mechanical and Energy Technology", Springer Science and Business Media LLC, 2020 Publication	<1 %
27	Potić, Ivan, Rajko Golić, and Tatjana Joksimović. "Analysis of insolation potential of Knjaževac Municipality (Serbia) using multi-criteria approach", Renewable and Sustainable Energy Reviews, 2016. Publication	<1 %
28	dk.cput.ac.za Internet Source	<1 %
29	Saeed Siah Chehreh Ghadikolaei. "Solar photovoltaic cells performance improvement by cooling technology: An overall review", International Journal of Hydrogen Energy, 2021 Publication	<1 %
30	worldwidescience.org Internet Source	<1 %

31	Ömer Faruk Can, Erhan Arslan, Meltem Koşan, Mehmet Demirtaş, Mustafa Aktaş, Burak Aktekeli. "Experimental and numerical assessment of PV-TvsPV by using waste aluminum as an industrial symbiosis product", Solar Energy, 2022 Publication	<1 %
32	Submitted to Marmara University Student Paper	<1 %
33	Submitted to Universidad Internacional de la Rioja Student Paper	<1 %
34	Submitted to Banaras Hindu University Student Paper	<1 %
35	Martin Raju, Rakesh Narayana Sarma, Abhilash Suryan, Prasanth P. Nair, Sandro Nižetić. "Investigation of optimal water utilization for water spray cooled photovoltaic panel: A three-dimensional computational study", Sustainable Energy Technologies and Assessments, 2022 Publication	<1 %
36	Submitted to University of Nottingham Student Paper	<1 %
37	V.V. Tyagi, S.C. Kaushik, S.K. Tyagi. "Advancement in solar photovoltaic/thermal (PV/T) hybrid collector technology",	<1 %

	Renewable and Sustainable Energy Reviews, 2012 Publication	
38	Vajjha, Ravikanth S., Debendra K. Das, and Dustin R. Ray. "Development of new correlations for the Nusselt number and the friction factor under turbulent flow of nanofluids in flat tubes", International Journal of Heat and Mass Transfer, 2015. Publication	<1 %
39	forum.dronebotworkshop.com Internet Source	<1 %
40	howtomechatronics.com Internet Source	<1 %
41	mountainscholar.org Internet Source	<1 %
42	research.wsulibs.wsu.edu:8080 Internet Source	<1 %
43	Submitted to Heriot-Watt University Student Paper	<1 %
44	Submitted to University of Petroleum and Energy Studies Student Paper	<1 %
45	www.repository.rmutt.ac.th Internet Source	<1 %
	stud.epsilon.slu.se	

46	Internet Source	<1 %
47	www.slideshare.net Internet Source	<1 %
48	Ioan Sarbu, Calin Sebarchievici. "Solar Collectors", Elsevier BV, 2017 Publication	<1 %
49	Sezgi Koçak Soylu, İbrahim Atmaca, Meltem Asiltürk, Ayla Doğan. " Improving heat transfer performance of an automobile radiator using and doped based nanofluids ", Applied Thermal Engineering, 2019 Publication	<1 %
50	www.scribd.com Internet Source	<1 %
51	www.thehindu.com Internet Source	<1 %
52	Usman Jamil Rajput, Jun Yang. "Comparison of heat sink and water type PV/T collector for polycrystalline photovoltaic panel cooling", Renewable Energy, 2018 Publication	<1 %
53	repository.sustech.edu Internet Source	<1 %
54	www.irjet.net Internet Source	<1 %

55	"Advanced Technologies for Solar Photovoltaics Energy Systems", Springer Science and Business Media LLC, 2021 Publication	<1 %
56	"Engineering Applications of Nanotechnology", Springer Science and Business Media LLC, 2017 Publication	<1 %
57	Bernardo Buonomo, Luca Cirillo, Oronzio Manca, Sergio Nardini. "Effect of nanofluids on heat transfer enhancement in automotive cooling circuits", AIP Publishing, 2019 Publication	<1 %
58	K.S. Muthukarupan, Santhosh Eashwar S, Vr. Subramanian, Sumit Tiwari, DB Singh. "Performance improvement of PVT module with applications of nano-fluids and phase change materials: A review", 2020 International Conference on Electrical and Electronics Engineering (ICE3), 2020 Publication	<1 %
59	Manju Santhakumari, Netramani Sagar. "A review of the environmental factors degrading the performance of silicon wafer-based photovoltaic modules: Failure detection methods and essential mitigation techniques", Renewable and Sustainable Energy Reviews, 2019 Publication	<1 %

60	Wei Pang, Yanan Cui, Qian Zhang, Gregory.J. Wilson, Hui Yan. "A comparative analysis on performances of flat plate photovoltaic/thermal collectors in view of operating media, structural designs, and climate conditions", Renewable and Sustainable Energy Reviews, 2020 Publication	<1 %
61	dspace.bracu.ac.bd:8080 Internet Source	<1 %
62	dspace.plymouth.ac.uk Internet Source	<1 %
63	eprints.utem.edu.my Internet Source	<1 %
64	ijesmr.com Internet Source	<1 %
65	myarduino.dk Internet Source	<1 %
66	researchcommons.waikato.ac.nz Internet Source	<1 %
67	worldradiohistory.com Internet Source	<1 %
68	Prabhat Chaurasia, Anil Kumar, Anshul Yadav, Praveen Kumar Rai, Virendra Kumar, Lalta Prasad. "Heat transfer augmentation in	<1 %

automobile radiator using Al2O3–water based nanofluid", SN Applied Sciences, 2019
Publication

69	Adrien Vogt-Schilb, Stephane Hallegatte. "Climate policies and nationally determined contributions: reconciling the needed ambition with the political economy", Wiley Interdisciplinary Reviews: Energy and Environment, 2017 Publication	<1 %
70	www.makerguides.com Internet Source	<1 %

Exclude quotes	On	Exclude matches	Off
Exclude bibliography	On		

ABBREVATIONS AND NOMENCLATURE

A	surface area (m^2)
C	specific heat (J kg^{-1} K^{-1})
E	electrical power output (W)
k	thermal conductivity (W m^{-1} K^{-1})
G	solar irradiation (Wm^{-2})
H	heat transfer coefficient (W m^{-2} K^{-1})
Nu	Nusselt number
Ra	Rayleigh number
Pr	Prandtl number
Pe	Perimeter (m)
Re	Reynold's number
T	Time (s)
m	mass (kg)
$\dot{m}$	mass flow rate (kg/s)
δ	Thickness (m)
α	Absorption coefficient
β	Solar cell temperature coefficient (K^{-1})
η	Efficiency
σ	Stefan Boltzmann constant, 5.670 x 10^{-8} (W m^2 K^{-4})
τ	Transmittance
Φ	Concentration of nano particles
Amb	ambient
GHG	Green House Gases
bf	base fluid
Env	environment
Con	convection
Cond	conduction
C	collector

Elec	electrical

CHAPTER 1: INTRODUCTION

1.1 Background and Motivation

PVT panels have hybrid output and produce thermal plus electrical output which will be used to pre-heat the water for the same covered area. This project directly relates to the Prime Ministers initiative of green eco-friendly sustainable energy production and automation. Environment damaging fossil fuels, natural gas and wood are being actively used in the local industry for water heating applications. This project will use clean and green solar energy to develop a complete automated water heating system.

This project directly addresses two priority areas, firstly Sustainable Energy and secondly Climate Change & Environment. Our proposed method not only addresses the issue of global warming but also focuses on the accuracy, functionality, scalability throughput, carbon footprint, resolution, and overalls cost effectiveness of the product by having a bespoke real-time feedback-controlled system which will bring economic benefit to a company.

The shortage of locally available fossil fuel along with its ever-increasing prices in the local market has put the local industry, in particular SMEs under intense pressure. The constant fluctuations in fuel rates and their ever-increasing price in the local market has forced the local industry to increase the price of their manufactured goods which has made the services, products, and parts of SMEs less competitive in the local as well as international market. One of the major hurdles being faced by the SMES is to control their cost of production which is directly linked to the cost of fuel prices. The unavailability of natural gas to the local industry due to its shortfall has also forced some of the local industry to use wood as an alternative source of fuel. Wood as a source of fuel is extremely harmful to the environment as it extracted by cutting down trees which causes deforestation, the

burning of wood causes direct emission of greenhouse gases which are a major contributor to global warming. In addition to the above as Pakistan is among the worst affected countries by climate change, it is imperative that the dependency on fossil-based fuels be minimized.

1.2 Problem Statement

The task is to design, fabricate and assemble a cost effective, sustainable, fully automated, and scalable water pre-heating/heating system using PVT solar plates.

1.3 Objectives

Following are the objectives of this project:

- Design and fabricate controlled hybrid water heating system using PVT plates.
- Improve electrical efficiency of PV plates.
- To make a fully automated system that heat water to a desired level.
- Development of scalable and cost-effective water pre-heating system.

CHAPTER 2: LITERATURE REVIEW

2.1 Conventional Fuels and their increasing prices

Depleting resources of natural gas in the country has already forced the governments to shift towards import of LNG and has created a hike in prices. In addition to an ever-increasing price of natural gas, due to a shortage in gas supply in the winter season when the demand of natural gas increases forces local governments to completely block the supply of natural gas for industries in order to cater for the domestic and commercial sector. This shortage in natural gas supply, its complete blockage for the industrial sector on very short notices for prolonged periods of time and its price has been detrimental for those SMEs who rely on it as a primary source of fuel for their manufacturing. This has resulted in a loss in business and forced some of the industries to shift towards the primitive method of using wood as a source of fuel to keep their business operational. Use of wood causes direct damage to the environment as it not only causes deforestation, but its use also creates greenhouse gases which cause global warming. Also, the efficiency of a wood-based boiler depends on the quality of wood and its moisture content at any given day which causes a fluctuation in the amount of wood required which is directly linked to the cost of production.

For the local SMEs and commercial entities who primarily rely on natural gas for heating have to shift towards sustainable and dependable solutions to keep their units running while protecting the environment.

The shortage of locally available fossil fuel along with its ever-increasing prices in the local market has put the local industry, in particular SMEs under intense pressure. The constant fluctuations in fuel rates and their ever-increasing price in the local market has forced the local industry to increase the price of their manufactured goods which has made the services, products, and parts of SMEs less competitive in the local as well as international

market. One of the major hurdles being faced by the SMES is to control their cost of production which is directly linked to the cost of fuel prices. The unavailability of natural gas to the local industry due to its shortfall has also forced some of the local industry to use wood as an alternative source of fuel. Wood as a source of fuel is extremely harmful to the environment as it extracted by cutting down trees which causes deforestation, the burning of wood causes direct emission of greenhouse gases which are a major contributor to global warming. In addition to the above as Pakistan is among the worst affected countries by climate change, it is imperative that the dependency on fossil-based fuels be minimized.

It is therefore imperative to address these concerns which are fundamental challenges being faced by the local industry. Small/Medium local industries are struggling to compete in the local as well as international market due to fluctuating and ever-increasing manufacturing costs and also because of having a large carbon footprint. Small scale industrial setups do not have neither the financial resources, nor the time and the technical R&D facilities (labs, software, technical knowledge, etc.) to develop a sustainable, reliable, automated, cost effective and environment friendly energy production solution.

2.2 Climate Change & Environment

Pakistan is in the list of the worst affected countries in the world by climate change [1]. Pakistan is ranked at 8th position in the list of countries most affected from climate change from 2000-1999 reported by German watch Global Climate Risk Index. According to the report, Pakistan has lost 0.52 percent per unit GDP, suffered economic losses worth US$ 3771.91 million and witnessed 173 extreme weather events from 2000 to 2019 [7].

CRI 2000-2019 (1999-2018)	Country	CRI score	Fatalities	Fatalities per 100 000 inhabitants	Losses in million US$ PPP	Losses per unit GDP in %	Number of events (2000–2019)
1 (1)	Puerto Rico	7.17	149.85	4.12	4 149.98	3.66	24
2 (2)	Myanmar	10.00	7 056.45	14.35	1 512.11	0.80	57
3 (3)	Haiti	13.67	274.05	2.78	392.54	2.30	80
4 (4)	Philippines	18.17	859.35	0.93	3 179.12	0.54	317
5 (14)	Mozambique	25.83	125.40	0.52	303.03	1.33	57
6 (20)	The Bahamas	27.67	5.35	1.56	426.88	3.81	13
7 (7)	Bangladesh	28.33	572.50	0.38	1 860.04	0.41	185
8 (5)	Pakistan	29.00	502.45	0.30	3 771.91	0.52	173
9 (8)	Thailand	29.83	137.75	0.21	7 719.15	0.82	146
10 (9)	Nepal	31.33	217.15	0.82	233.06	0.39	191

Figure 1: Top 10 countries affected from 2000 to 2019 (annual averages)

Over the last few years, Pakistan is among the countries that are frequently affected by calamities and is constantly ranked among most impacted countries.

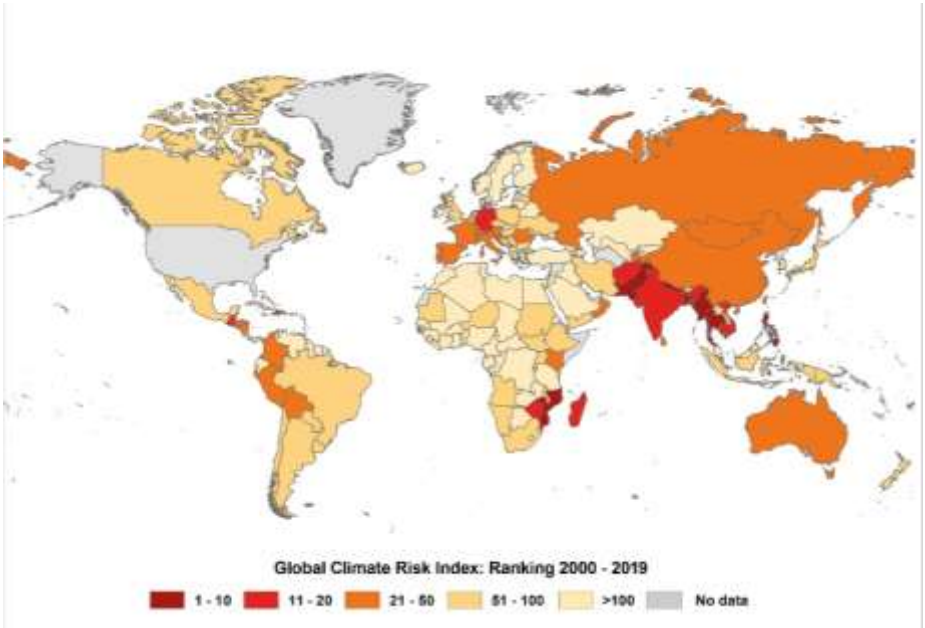

Figure 2: Global Climate Risk Index

Pakistan is already facing the unfavorable impacts of climate change. Two instances of these are the drought in 1998-2001 and the flood that country faced in 2010. 25 million individuals were affected by the later and it cause the loss of 9.5 billion US dollars [1]. Due to the extreme change in weather pattern, these are probably going to increase. The effects will hit all three aspects of sustainable development—environmental, social as well as economic.

Green House Gases emissions in Pakistan is probably going to rise for two reasons (1) development in agriculture, energy utilization and industry (2) Pakistan's future energy production is dependent on coal. National Economic and Environmental Development Study (NEEDS) anticipated Green House Gases Emissions (million tons CO2 eq.) to increment from 347 to 4621 from 2011 to 2050. Energy Sector will be the main contributor with almost 60 % share, followed by agricultural sector [1].

Climate change will have significant economic consequences. It will affect water security, food security and energy security. It will also disturb agricultural sector, forestry, cattle, and fisheries, among other sectors crucial to the economy of Pakistan.

Climate change will have a negative impact on health, lead people to be displaced, and result in a loss of income as a result of increased natural disasters i.e., flood, droughts, and sea level rise. It might threaten hundreds of jobs, cause increase in food price, and raise the number of people facing food insecurity and famine. It might also lead to migration and displacement, as well as civil unrest.

Changes in ecology and habitats, as well as the quality and amount of land, soil, water, and biological reserves, as well as rises in the level and temperature of sea and salinity, are all anticipated to be severe consequences of climate change. It might also lead to the spread of weeds and pests, that might worsen detrimental changes in environment [1].

The extremely high dependency of Pakistan on fossil fuels, natural gas, and wood as a source of fuel has to be reduced as these fuels cause the emission of Green House Gases which are bringing a constant change in temperatures throughout the country [2].

To combat climate change and its negative consequences, world leaders in Paris agreement pledged to lower greenhouse gas emissions to keep global warming well below 2 $^{\circ}$C, preferably 1.5 degrees Celsius.

2.3 Solar Energy

Solar energy is an ecofriendly, renewable and freely available source of energy. Its usage will enable the conservation of other energy sources while also protecting the environment from damage. Solar energy appears to be the most promising and sustainable renewable source of energy among all the other sources. As a result, systems based on solar energy can fulfil certain energy demands while still maintaining ecological balance. Solar radiation can be transformed into thermal, electrical, or both types of energy [3].

2.4 Photovoltaic (PV) Panels

Photovoltaic (PV) technology is the most efficient technique to convert solar energy into electricity. Solar cells are photoelectric energy conversion devices that employ the photoelectric effect to convert sunlight to electricity. Solar cells and ancillary components make up a photovoltaic system. It directly converts solar radiation into electricity. In 1954, researchers used a p–n junction cell with a 6 percent efficiency to convert solar energy into electric energy [5]. Now a days, solar power conversion efficiency is typically between 15 and 20%. [6].

2.4.1 Effect of Temperature on performance of PV cell

Output electrical energy of PV system is just a fraction of the incoming solar energy, and this is how their efficiency is measured. Meanwhile, most of the energy is lost as heat.

Upgrading of Photovoltaic cell technology is a very active subject of research in order to reduce energy losses and boost module efficiency. At research level the best cell efficiency is achieved by NREL of 47.1 percent ± 2.1 by utilizing a multi-junction terrestrial concentrator cell built with AlGaInP/AlGaAs/GaAs/GaInAs layers [9,10]. The most extensively used commercial technology is Si-based PV technology. Kaneka Corporation's best research level cell efficiency attained is 26.7 percent 0.5 ± percent [10,11]. However, there is always a significant gap between research and commercially accessible module efficiency, as well as already installed panels. Furthermore, these efficiencies are assessed at STC, in which the cell temperature is considered at 25 degrees Celsius. In practice, however, this is not always the case since the temperature of the cell rises owing to heat dissipation from wasted irradiant solar energy that is not transformed into electrical energy production.

The output electrical power of Si PV cells drops by around 0.5 percent for every 1°C increase in cell temperature [12]. This loss is substantial at greater solar irradiance and ambient temperature, and can approach 75 °C, resulting in a 25% reduction in efficiency in comparison to STC value [13].

Furthermore, higher cell temperatures lower the lifespan of PV panels [14]. With every 10 °C rise in temperature of solar cell, the ageing rate of PV modules is projected to double [15].

This decrease in module lifetime and operational efficiency result in large losses of electrical energy and profit, which is an issue for both present and novel PV cell technologies.

Hence the decrease of PV cell temperature is highly beneficial [16]. We can use recovered heat for practical applications i.e., for heating and cooling Buildings, in the water heater, and it can be used to dry some foods and by achieving moderate operating temperatures

for PV panels we obtain higher electrical efficiency in comparison to conventional PV panels.

2.5 Solar Thermal Energy Collector

Another Technique of using solar energy is with Solar thermal energy collectors. These can be considered as heat exchanger which uses a transport medium and/or a moving fluid to convert solar radiation into thermal energy. The most important part of the system is the solar collector. It collects solar radiation, transforms it to heat energy, and transmits it to beneficial purposes/applications through some fluid (typically air, water, or oil) [4].

2.6 PVT Hybrid Solar Technology

PVT panels are mainly constructed by using a typical thermal collector and by covering its absorber with an appropriate Photovoltaic (PV) layer. The thermal energy is circulated through a fluid which is typically air [17] or water [18], whereas the PV top layer generates electrical energy [19]. The net overall result of this technology is the production of both thermal heat and electrical energy [20], with a increase in the electrical efficiency of the top PV module. The efficiency of conventional PV panels has been known to drop with increase in temperature of the PV module, this decrease in efficiency corresponds to a decrease in the output electrical production. PV Cells consume a segment of the incident solar energy to generate electrical power as output whereas the remaining incident solar energy is converted into waste heat in the cells, this results in a raise in temperature of the PV module, resulting in a decrease in efficiency of the module [20]. The hybrid PVT technology recovers part of this heat which can be used for practical applications. By achieving moderate operating temperatures for PV panels, it is possible to obtain higher electrical efficiency in comparison to conventional PV panels as well [21,22].

2.6.1 Transport fluid options

Heat can be transferred by liquid or air in flat plate collectors.

Due to its accessibility and appropriate thermal qualities, water is a popular option as a liquid fluid:

- It has an astronomically high capacity for volumetric heat.
- It can't be squished (or nearly incompressible)
- Its mass density is abnormally high (which lets in the usage of small tubes and pipes for transport)

Water has the disadvantage of freezing throughout the winter, which can cause damage to the collector or pipe system. Low photovoltaic inputs can be controlled by emptying the collector (below an indispensable insolation threshold). Water freezing can cause harm, thus drain down sensors are commonly used to uncover the device and ensure complete emptying. Air pockets in the heat collector can be a problem, water which floats block and reducing gadget effectivity [3].

Antifreeze combinations can be used instead of clean water to solve the difficulties mentioned above. Ethylene glycol and propylene glycol are common antifreeze components. Due to the toxicity of these chemical compounds when coupled with water, closed-loop structures and proper disposal are required. A typical antifreeze supplier lasts around 5 years before needing to be replaced [4].

In some flat-plate collector systems, air may be employed as a transport fluid. This option is better suited to heating a large area or drying crops. A fan is usually necessary to allow air to float in the machine and to transfer heated air in an environmentally acceptable manner. Due to thermal buoyancy, certain designs can provide passive (non-fan) air motion [4].

Also, phase-change fluids can be utilized to prevent water freezing. These fluids have a low boiling point, which can help them transition from liquid to gasoline when the temperature gets higher. These could be useful in situations with rapid reaction.

2.6.2 Nanofluids

Due to the increasing need for high-efficiency engines, the need for cooling systems has become more prevalent. One way to improve the cooling capacity of a radiator is by using fins.

Unfortunately, warmth switch fluids, which include water and ethylene glycol, have a poor thermal conductivity. This makes them unsuitable for use in cooling systems. New and innovative technologies are needed to improve the efficiency of the cooling system by introducing warmth switch fluids.

Recently, it has been proven that nano-based warmness switch performances are the most reliable. In a cooling system, a team of researchers utilized copper nanofluids and ethylene glycol as a base fluid. They found that the combination of these two fluids increased the warmth switch parameter [25]

Copper nanofluids serve as a base fluid, and ethylene glycol serves as a solvent. They discovered that the warmth switch coefficient increased when compared to the basic fluid. When they looked at the Reynolds ranges of 6000 and 5000 for air and coolant, they discovered that a 2% increase in quantity awareness increased the warmth switch by 3.8 percent. They've also supplied several markers of deterioration of the frontal surface. Hussein and his colleagues [16].

To test the expansion of a warming switch, the oxides of silicon and titanium were utilised in stream line flow conditions with 100 percent water. The float rate, intake heat, and the observations of transferring fluid are all between two and 8 liter per minute, sixty to 80°C, and upto 2 percent. The worldwide warmness switch parameter of aluminum oxide and ethyl glycol fluid, which was utilised as a cooling fluid in a vehicle under stream line, was subject of Subhedar's study [27]. The experimental setup resembles a car's cooling system.

A two-step process was used to form the nanofluid, which comprised employing ultrasonic to disperse for the aluminum oxides and copper oxide fluids. Use of nanofluid increases the global warmness switch coefficient when compared to the base fluid, according to the results of the experiments. The normal warmness switch coefficient is increased by raising the volumetric awareness of nanoparticles from 0% to 8%. The input temperature varies from 65 to 85 degrees Celsius.

Finally, researchers observed that transferring fluid having awareness 2% Al2O3 may reduce the warmth exchanger floor by upto thirty seven percent [28]. It have conducted a calculated evaluation of the CuO-water nanofluid's utility in an automobile diesel engine radiator. Under specific conditions, the warmth switch coefficient and pumping energy for fluid of two percent attention running through perfect straight collector at 70 km/hr were roughly 10% and 23.8 percent greater than the basic fluid.

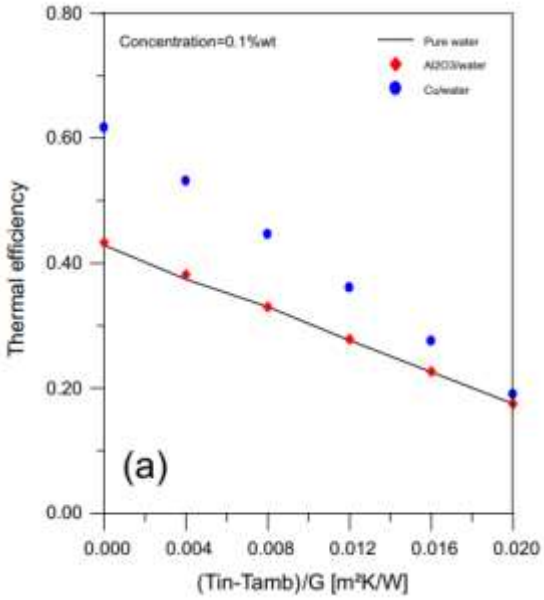
Concentration=0.1%wt
Pure water
Al2O3/water
Cu/water
Thermal efficiency
(Tin-Tamb)/G [m²K/W]
(a)
0.80
0.60
0.40
0.20
0.00
0.000
0.004
0.008
0.012
0.016
0.020

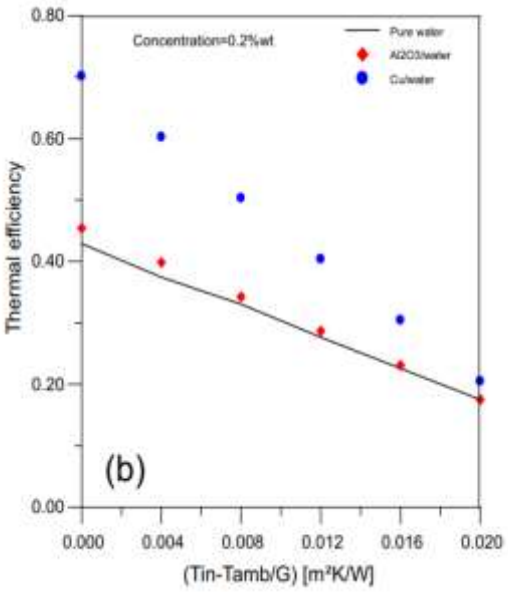
Concentration=0.2%wt
Pure water
Al2O3/water
Cu/water
Thermal efficiency
(Tin-Tamb/G) [m²K/W]
(b)
0.80
0.60
0.40
0.20
0.00
0.000
0.004
0.008
0.012
0.016
0.020

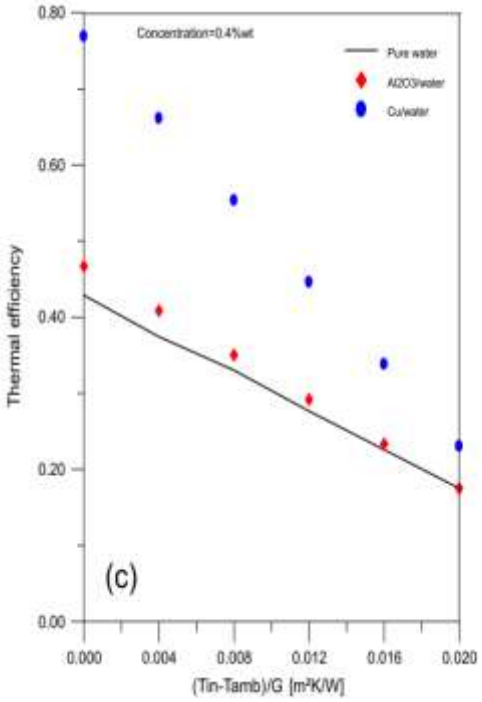
Concentration=0.4%wt
Pure water
Al2O3/water
Cu/water
Thermal efficiency
(Tin-Tamb)/G [m²K/W]
(c)
0.80
0.60
0.40
0.20
0.00
0.000
0.004
0.008
0.012
0.016
0.020

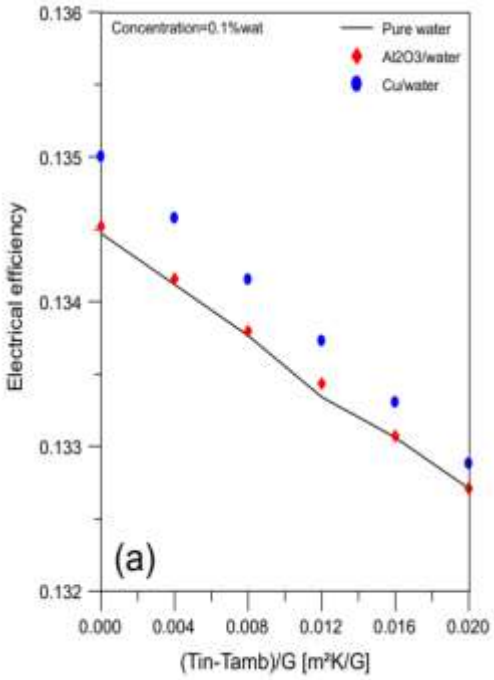
Concentration=0.1%wat
Pure water
Al2O3/water
Cu/water
Electrical efficiency
(Tin-Tamb)/G [m²K/G]
(a)
0.136
0.135
0.134
0.133
0.132
0.000
0.004
0.008
0.012
0.016
0.020

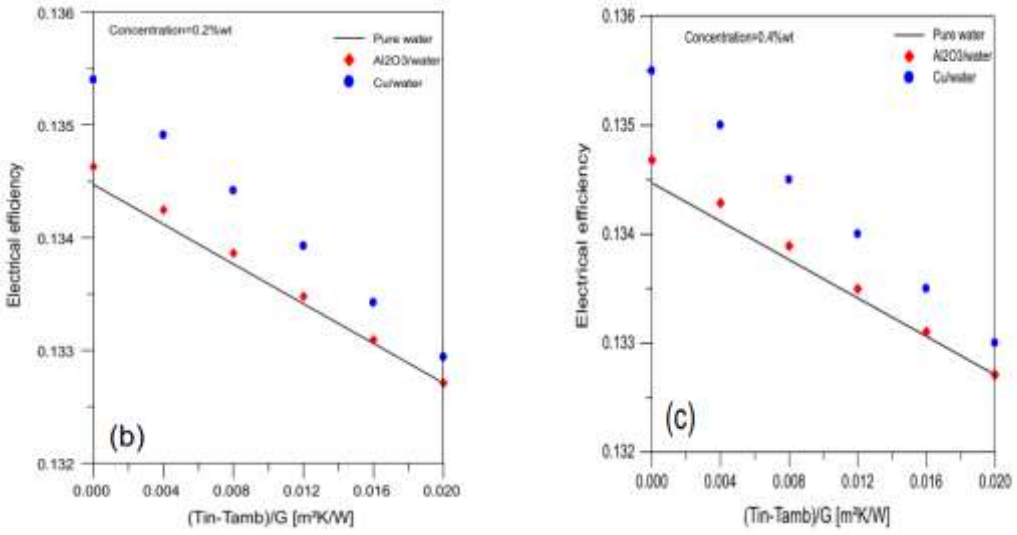

Figure 3: Effect on electrical efficiency by nanofluids

The convective warmth switch coefficient is connected to the drift speed and inversely proportionate to the drift temperature, according to the findings. The warmth switch is 78.67 percent greater than the typical fluid in an automotive radiator. Elbadawy [29] investigated the thermal and flow characteristics of transferring fluids of oxides of copper and aluminum flowing in straight collector. The warmness switch coefficient increased by 45 percent also thirty eight percent for oxides of copper and aluminum, when observed with pure water. The most reliable nanoparticle quantity attention is investigated, which supplies a moderate warmness switch enhancement with a moderate pumping strength increase.

CHAPTER 3: METHODOLGY

PVT collectors mix the era of photo voltaic electrical energy and warmth in a single component, and as a result obtain a greater common effectivity and higher utilization of the photo voltaic spectrum than traditional PV modules.

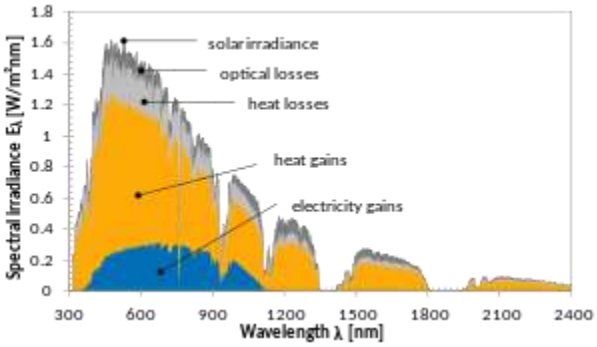

Figure 4: A PVT spectrum

The general perspective is to be the efficiency of PV module electrically is about to be 15-20% but about 70% of the solar radiations are converted in the heating of the solar panels. The photovoltaic collectors on the other hand are designed to collect the heat from the solar radiations to a thermal fluid which cools down the temperature and also the efficiency of the solar plate increases. The result of the cooling of the plates is first of all the efficiency of the solar plate is increased and the feed to the pump is also the cooled water. As the result the solar collectors are the heat wasted by the solar radiations to the most efficient.

The solar cells temperature is the rise in the temperature of the silicon biased cells and this rise in temperature reduces the efficiency in results. The reason by which the solar cells efficiency is reduced by 0.2-0.5% with every change in the kelvin of the rise in the temperature. The results of the lowering the temperature of the photovoltaic cells is the increase in the electrical efficiency of the PV cells. Every single benefit of the lowering the temperature of the cells is increasing the lifetime of the solar panel.

This is a good way to increase the overall reliability of the machine and the efficiency, but the effects of the use of hybrid thermal element is the effectivity of the thermal collector decreases. The reason of seeing the maximum objectives of getting the best possible output from PVT devices is from below 100 degrees Celsius and the temperature at which a cell can work is also below 100. Then depending upon the cells efficiency and gadget designs for each and every electrical unit we have cooling devices for the better efficiency.

3.1 Model for mathematics

The heat transfer in the plates of the different layers of the PV panel and the every plate such as the panel, heat absorber, collector tubes and the fluid in the tube which can be water or nanofluids and then the insulation, these things are described by the order as such described above and the thermal and electrical efficiencies are observed on the covered and uncovered plates shown in Fig. 1 shows complete description in the layers of the plate and heat collector. A portion of the incident photovoltaic radiation is converted to electrical power and the rest is converted to heat by the solar module. Al2O3/water (H2O), Al2O3/ethylene glycol (EG), Cu/H2O, and Cu/ethylene glycol (EG) were used in this research (EG). Table 1 summarises the thermophysical properties of the mentioned nanofluids. A thermal insulation (fibreglass) is positioned at the lower rear of the PV/T collector to minimise the warmth losses from the absorber and tubes. Some assumptions are taken into account in the numerical simulation to make calculations easier:

• In tubes, the cost of nanofluid drift is consistent.

• The PV plate, absorber layer, collector tubes and insulation all have the same thermo-physical properties.

• The sky is depicted as a dark body. The collector elements' electricity stability equations are represented using these assumptions as a basis.

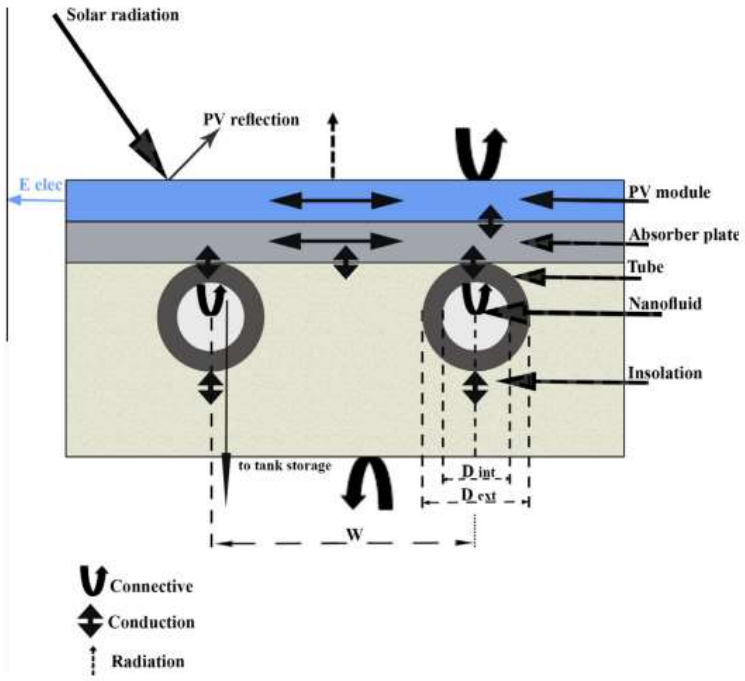

Figure 5: Uncovered nanofluid type photovoltaic collector

Table 1: Model for mathematics

	p (kg m^{-3})	C_p ($Jkg^{-1}K^{-1}$)	K($Wm^{-1}K^{-1}$)
Pure water	997.1	4179	0.613
Pure ethylene glycol (EG)	1113.2	2470.2	0.258
Copper (Cu)	8933	385	401
Alumina (Al_2O_3)	3970	765	40

3.1.1 PV module thermal balance

The heat transfer of the PV module is said to be the total heat gained by the solar plate module from the solar radiations strike on the plates minus the total heat transferred to the absorber plate, the transferred radiations are to be change by the time in the day as we know such like this we also know the electricity gained also change by this radiation change, as determined by the thermal stability of the photovoltaic module.

$$m_{pv}C_{pv}\frac{dT_{pv}}{dt} = \alpha_{pv}G + A_{pv,env}h_{ray,pv\to env}(T_{sky} - T_{pv}) + A_{pv,amb}h_{wi}(T_{amb} - T_{pv}) - E_{elec} + A_{pv,pab}h_{cond,pv\to pab}(T_{pab} - T_{pv}) + A_{pv}k_{pv}\left(\frac{\partial^2 T_{pv}(x,y)}{\partial x^2} + \frac{\partial^2 T_{pv}(x,y)}{\partial y^2}\right) \quad (1)$$

the spot The mass and exact warmness of a PV module are represented by mPV and CPV, respectively. aPV is the PV module's absorptivity coefficient; G is the photovoltaic radiation absorbed in the collector; hray,PVenv, and hwi are the radiation and convection warmth switch coefficients at the PV module's pinnacle; hcond,PVpab is the conduction warmth switch coefficient between the PV module and the absorber plate; Tpab, Tsky, and Tamb are the temperature of the absorber plate, sky Finally, Eelec is the electrical output strength created by photovoltaic cells.

3.1.2 The absorber plate's thermal equilibrium

The inner power trade of the plate can be used to determine the thermal stability of the absorber plate. It's the sum of the strength transferred from the plate absorber to the tube and the power transferred from the absorber plate to the insulation minus the strength switch from the absorber plate to the photovoltaic module.

$$m_{pab}C_{pab}\frac{dT_{pab}}{dt} = A_{pv,pab}h_{cond,pv\to pab}(T_{PV} - T_{pab}) + A_{pab,tu}h_{cond,pab\to t}(T_{tu} - T_{pab}) + A_{pab,i}h_{cond,pab\to i}(T_i - T_{pab}) + A_{pab}k_{pab}\left(\frac{\partial^2 T_{pab}(x,y)}{\partial x^2} + \frac{\partial^2 T_{pab}(x,y)}{\partial y^2}\right) \quad (2)$$

a location The mass and exact heat of the temperature of absorbing plate, respectively, are represented by mpab and Cpab. The conduction heat transfer in the plates for absorbing heat is $h_{cond,pabt}$, and the conduction in the plate for absorption and also in the insulation is $h_{cond,pabi}$. The collector tubes and the ins temperature are denoted by the letters T_{tu} and T_i. The plates for absorption and the collector tube make contact at apab.tu. The following is a rough estimate [1]:

$$A_{pab,tu} = \delta_{pab}L$$

$$A_{pab,tu} = 0.0015 \times 5.9436$$

$$= 0.0297m^2$$

The δ_{pab} = 0.0015m and L = 5.9436m are the parameters for the thickness and length of the tube respectively.

$$A_{Pav,Pab} = 0.46 \times 0.62$$

$$= 0.2852\ m^2$$

The contact area between the insulation and the absorber plate is represented by $A_{pab,i}$. It can be calculated as follows [1]:

$$A_{pab,i} = A(W - D_0)/W$$

$$A_{pab,i} = 0.2852(0.02-0.009525)/0.02$$

$$=0.14937m^2$$

Where we have A and D_0 are the spacing of tube and the outer diameter of the tube respectively.

$$h_{cond,pv\rightarrow pab} = k_{ad} / \delta_{ad}$$

$$=1.28 / 0.0005$$

$$=2560\ J/kg.K$$

As k_{ad} and δ_{ad} are adhesive thermal conductivity (1.28 W/m.K) and thickness of adhesive layer (0.5mm).

$$h_{cond,pab\rightarrow t} = 2k_{pab} / ((W-D_o)/4)$$

$$=2(310)/ (0.02-0.009525)/4$$

$$= 236754.176\ J/kg.K$$

As k_{pab} ,W and D_o are absorber plate thermal conductivity (310) , spacing of tubes(0.02m) and outer dia of tubes (0.009525m) respectively.

$$h_{cond,pab\rightarrow i} = 2k_i / \delta_i$$

$$= 2 \times 0.136 / 0.05$$

$$= 5.44$$

As k_i and δ_i are thermal conductivity of insulation (0.136 W/mK) and thickness of insulation (2cm) respectively.

So, the final energy balance of the absorber plate become

$$\Delta U_{pab} = A_{pav,pab}\, h_{cond,pv\rightarrow pab}\,(T_{pv} - T_{pab}) +$$

$$A_{pab,tu}\, h_{cond,pab\rightarrow t}\,(T_{tu} - T_{pv}) +$$

$$A_{pab,i}\, h_{cond,pab\rightarrow i}\,(T_i - T_{pab}) + 0$$

$$\Delta U_{pab} = 730.12(T_{pv} - T_{pab}) + 7031.6(T_{tu} - T_{pv}) + 0.8125(T_i - T_{pab})$$

The last term is ignored as we take the readings at the following conditions as

The uniformity of the temperature in the plates and the absorber layer and the insulation.

The flow is laminar and the temperature distribution is uniform.

3.1.3 Tube's thermal equilibrium

The tube's thermal stability can be estimated by calculating the inside power trade as the conduct electricity transfer from the collector to the ins and heat travel from the collector to the fluid in the collector and then the heat is travelled from the collector to the insulation installed.

$$\begin{aligned}\rho_{tu}\delta_{tu}PedyC_{tu}\frac{dT_{tu}}{dt} &= A_{pab,tu}h_{cond,pab\rightarrow tu}(T_{pab} - T_{tu}) \\ &+ Peh_{conv,tu\rightarrow f}dy(T_f - T_{tu}) + A_{i,tu}h_{cond,tu\rightarrow i}(T_i - T_{tu}) \\ &+ k_{tu}\delta_{tu}dyPe\left(\frac{\partial^2 T_{tu}}{\partial^2 y}\right) \qquad (3)\end{aligned}$$

Density, thickness, exact warmth, and temperature of the tube are all represented by the units q_{tu}, d_{tu}, and C_{tu}. The temperature of a nanofluid is denoted by the symbol T_{nf}. The same zone between the collector and the insulation is designated by the letters a_{tu},i. The following equation [1] can be used to determine this:

$$A_{tu;i} = D_0 L(\pi/2 + 1)$$

$$= 0.009525 \times 5.9436\,(\pi/2 + 1)$$

$$= 0.1455 m^2$$

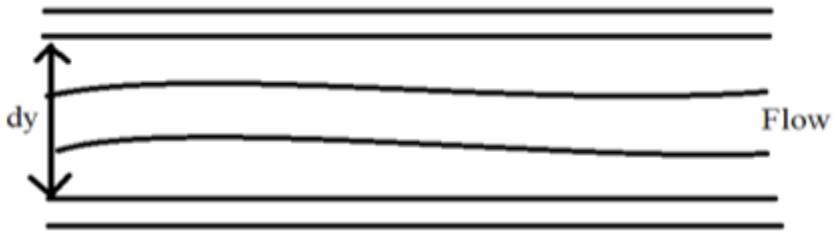

Figure 6: Flow in tube

The internal energy change of the tube is

$$= A_{pab,tu}\, h_{cond,pab\rightarrow t}\, (T_{pv} - T_{tu}) + Pe.\, h_{conv:tube}\, dy(T_f - T_{tu})$$

Where dy is internal dia of the tube and the perimeter of the whole tube at back of the solar panel is Pe and $h_{conv:tube}$ is h as follow

$$h = Nu.k / D$$

This is the only expression exist if and only if the following conditions are followed

- The tubes are perfectly circular and of continuous cross-section.
- Fully developed laminar flow.
- Constant flow conditions.

The first condition is laminar flow is justified by Reynold's number as follow

$$Re = pVD/\mu$$

As Q=AV so V=Q/A

$$=998 \times Q/A \times 0{,}009525 / 0.001003$$

$$So,\ V= 1.8 \times 1.662 \times 505 / 3.14(0.009525/2)^2$$

$$V=0.421\ m/s$$

And

$$Re = 3390$$

This Reynold's number is for the maximum speed of fluid passing in tubes if the speed decreases the laminar flow will be maintained as it is as Reynold's number decreases.

So the $h_{conv:tube}$ is calculated by

$$Nu = hD/k = 4.36$$

$$h = 4.36 \times 0.613 / 0.009$$

$h = h_{conv:tube} = 296.96\ W/m^2K$

And dy is the inner diameter of the copper tube which is 0.009m and calculations for perimeter is as follow

The inner perimeter of the tube is

$Pe = 2(L+W)$

Where L is circumference of cylinder inner circle and

W is the total length of the tube

So

$Pe = 2(2\pi R + H)$

$Pe = 2(\pi(0.009) \times 5.9436)$

$= 11.9472m$

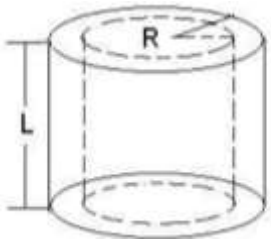

So, the final equation for internal energy of tube is

$= A_{pab,tu}\ h_{cond,pab \rightarrow t}\ (T_{pv} - T_{tu}) +$

$Pe.\ h_{conv:tube}\ dy(T_f - T_{tu})$

$= 7031.6(T_{pv} - T_{tu}) + 319.30(T_f - T_{tu})$

3.1.4 Transferring Fluid

The energy transfer in the transferring fluid is described below:

$$\rho_{nf} A_{nf} dy C_{nf} \frac{dT_{nf}}{dt} = Peh_{conv,t \rightarrow nf} dy(T_t - T_{nf}) - \dot{m} C_{nf} \Delta T_{nf} + k_{nf} \delta_{nf} \left(\frac{\partial^2 T_{nf}}{\partial^2 y} \right) \quad (4)$$

The symbols qnf, m, and Cnf of the transferring fluid. For heat transfer, the nano fluid used is Water. The final time period associated with the conductive warmth switch may want to be as short as possible.

3.1.5 Insulation

The insulation's thermal stability can be expressed by considering that the insulation's inner variant power, electricity transferred from the module to absorbing panel then to semiconductor insulated sheet and then from collector to insulated sheet, except lost in atmosphere.

$$m_i C_i \frac{dT_i}{dt} = A_{tu,i} h_{cond,tu\to i}(T_{tu} - T_i) + A_{pab,i} h_{cond,pab\to i}(T_{pab} - T_i) + A_i h_{wi}(T_{amb} - T_i) + A_i k_i \left(\frac{\partial^2 T_i(x,y)}{\partial x^2} + \frac{\partial^2 T_i(x,y)}{\partial y^2} \right) \quad (5)$$

the place m_i and C_i are the mass and precise warmness of insulation, respectively. The warmth switch coefficients that are utilized in electricity stability equations (cited above) are given as:

– Conv heating Parameter:

Temperature is also given to the collector from the heat get from the radiations denoted by, h_{wi}, is rely on air speed, Mc Adams gave an equation. This equation is used in this paper [2]

$$h_{wi} = 5.7 + 3{:}8V_{wi} \quad (6)$$

Relation used for estimation:

$$h_{conv,tu\to nf} = Nu_{nf} k_{nf} / Dia \quad (7)$$

where the thermal conductivity of the water is k_{nf} and diameter of the tube is Dia. Nu_{nf} is the Nusselt number.

3.1.6 Conduction heat transfer coefficients

The coefficient of heat transfer between two adjacent layers can be expressed by the following relationship [3]

$$h_{cond,m\to n} = \frac{1}{\frac{\delta_m}{k_m} + \frac{\delta_n}{k_n}}$$

The following equation may be used to represent the conduction heat transfer coefficient between the PV module and the absorber plate, $h_{cond,pvpab}$[4].

$$h_{cond,pv\rightarrow pab} = k_{ad}\, d_{ad}$$

where d_{ad} and k_{ad} are the adhesive's thickness and heat conductivity. Flows [1] may be used to calculate the conduction heat transfer coefficient between the absorber plate and the tube, $h_{cond,pabtu}$

$$h_{cond,pab\rightarrow tu} = 2k_{pab} /((W\text{-}D_0)/ 4)$$

Flows [1] may be used to calculate the conduction heat transfer coefficient between the absorber plate and the insulator, $h_{cond;pab,t}$.

$$h_{cond,pab\rightarrow i} = 2k_i /d_i$$

Nanofluid thermal and physical properties Maxwell [6] proposed a relationship for calculating nanofluid thermal conductivity (which is used in the present work). It is determined by the base fluid's thermal conductivity, as well as the concentration of nanoparticles.

$$k_{nf} = \frac{[(k_{n,p} + 2k_{bf}) + 2\phi + (k_{np} - k_{bf})]}{[(k_{n,p} + 2k_{bf}) - \phi(k_{np} - k_{bf})]}$$

3.1.7 Activating Parameters

Initially, the photovoltaic module, tube, and insulation temperatures are considered to be constant and equivalent to the ambient temperature.

$$T_{pv}\,(t = 0),\ T_{tu}\,(t = 0),\ T_i\,(t =0) = T_{amb}$$

The assumption is made at start the temperature of water is initial temperature of water:

$$T_{nf}\,(t = 0) = T_{in}$$

3.1.8 Studying Energy

The usable acquired energy by the collector from incoming solar radiation (Eq. (15) may be stated as the thermal efficiency of the PV/T collector.

$$\eta_{th} = \dot{m}C_{p,nf}(T_{out} - T_{in}) /A_cG$$

Mass drift rate, photovoltaic radiation, specific warmth of the nanofluid, and collector floor position are all represented by the letters G, Cp,nf, and Ac, respectively. Evan et al. [8] developed an empirical relationship that may be used to assess the electrical effectivity of a solar unit. It is inversely proportional to the temperature of the cells, and it is defined as follows:

$$\eta_{elec} = \eta_0[1 - \beta(T_{pv} - 298)]$$

where η_0 and β are the photoelectric efficiency at the initial condition and the cells temperature coefficient respectively.

3.2 Properties used in simulation:

The properties use in the simulations are give in the tables below.

Table 2: Thermophysical properties of some fluids used

	p(kg/m^3)	C_p (J/kg. K)	K(W/mK)
Pure water	998	4179	0.613
Pure ethylene glycol	1113.2	2470.2	0.258
Copper (Cu)	8933	385	401
Alunina (Al_2O_3)	3970	765	40

Table 3: The properties of Photovoltaic panel

Open Circuit voltage	I_{oc} = 0 A	V_{oc} = 20.6V
Short Circuit Current	I_{sc} = 2.57 A	V_{sc} = 0V
Maximum Power output	I_{mp} = 2.29 A	V_{mp} =17.4V

Table 4: The collector Parameters applied in simulation

Components	Parameters	Value	Unit
PV module	Specific Heat,C_{pv}	900	J/kg.K
	Thermal Conductivity,K_{pv}	140	W/mK
	Emissivity	0.93	
	Reference cell efficiency,$\eta_\circ$	15	%
	Packing Factor, Pac	0.8	
Absorber Plate	Density, p_{ab}	2702	Kg/m^3
	Thhermal Conductivity,k_{pab}	310	W/mK
Tube	Density, p_t	2702	Kg/m^3
	Thhermal Conductivity,k_t	310	W/mK
	Tube number	16	
	Diameter of tube,D	0.0095	m
	Thickness, δ_t	0.00025	m
Insulation	Thickness, δ_i	0.05	m
	Density, p_i	45	Kg/m^3
	Thermal Conductivity,k_i	0.136	W/mK
	Specific Heat,C_i	835	J/kg.K

3.3 The Heat transfer in tank by coil

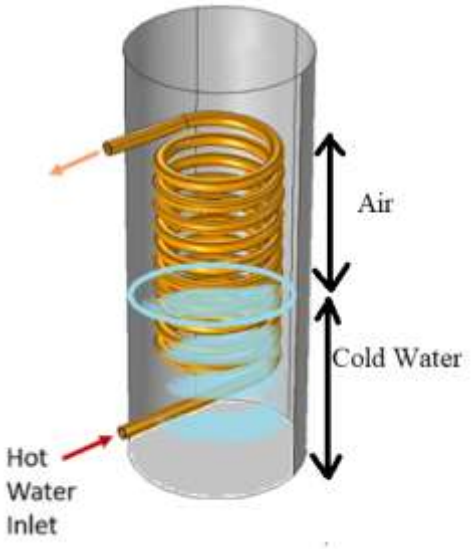

Figure 7: Heat transfer in tank by coil

The heat transfer in the tank is done by the coil in the tank which is half cooled by water and second half by air as shown in the above figure.

Shell heat exchangers are the most common form. A copper coil is made up of a duct that transports cold air and heats it.

In the Convective Heat Flux border scenario, a Nusselt extent correlation for induced internal convection is used to calculate the warmness change between the water and copper tubing. At all of the copper piping's indoor boundaries, this boundary condition is employed. As inputs, it takes into account pipe diameter, fluid type, fluid velocity, and fluid temperature. Between tube twists, all of these components, with the exception of the fluid temperature, continue to operate correctly.

3.4 Thermodynamic Modeling of Temperature Drops Between Turns:

The copper coils cool the hot water as it is pushed. Due to the axisymmetry of the model, each coil turn is independent of the others unless we expressly omit data between them. That is, at the internal borders of each coil turn, we must comply with a different Convective Heat Flux boundary scenario.

This raises the question of how we can compute and incorporate the temperature drop between each flip in our calculations.

Consider the water passing through one of the copper coil's rounds. The heat transferred into the copper pipes is equivalent to the heat lost by the water's ability to conduct heat. The temperature decrease of water travelling through one turn of the pipe, with normal fabric characteristics and no viscous losses,

$$\Delta T = \frac{Q}{\dot{m}C_p} = \frac{\int q'' dA}{\dot{m}C_p}$$

where is the mass drift rate, is the special warmness of water, and is the complete warmness misplaced by way of the water, which is equal to the essential of the warmness flux into the copper, built-in over the internal boundaries of the coil. This critical can be evaluated with the useful resource of the Integration Component Coupling, described over the inside coil boundaries.

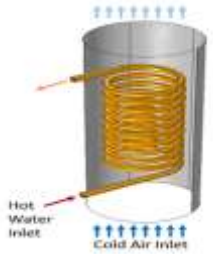
Hot
Water
Inlet
Cold Air Inlet

3.5 Heat Exchanger used:

We have taken relatively simple design to transfer the heat taken from the panel to the water present in the tank which will transfer heat by mare conduction

Copper Tube to Air:

The calculation for the heat transfer is simply

$$Q \text{ dot} = \dot{m} \times C_p \times \Delta T$$

Where:

- $\dot{m}$ is mass flow rate of water or nano fluid in the tube
- C_p is the specific heat of the water or nano fluid in the tube
- ΔT is the temperature difference of the tube water or nano fluid in the air.

And if we divide this Q dot with the Area of the tube present in the air is the value of flux that the heat transfer in the air by copper tube per unit area in unit time.

Copper Tube to Water:

The calculation for the heat transfer is simply

$$Q \text{ dot} = \dot{m} \times C_p \times \Delta T$$

Where:

- $\dot{m}$ is mass flow rate of water or nano fluid in the tube
- C_p is the specific heat of the water or nano fluid in the tube
- ΔT is the temperature difference of the tube water or nano fluid in the water.

By this we can find the heat transferred by the copper tube in the water as per the temperature change in the in the copper tube and the flow rate as these parameters are known to us or we can find these by the sensors applied in the project.

And if we divide this Q dot with the Area of the tube present in the water is the value of flux that the heat transfer in the air by copper tube per unit area in unit time in water.

3.6 Reference Results

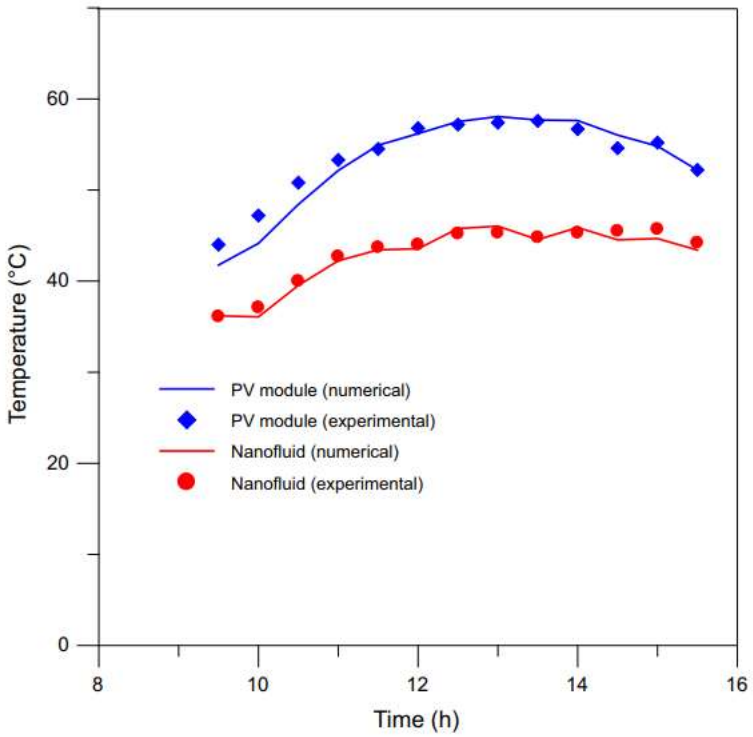

Figure 8: The Reference results of temperature change with time in experimental and theoretical way

Where Nanofluid used is **Water.**

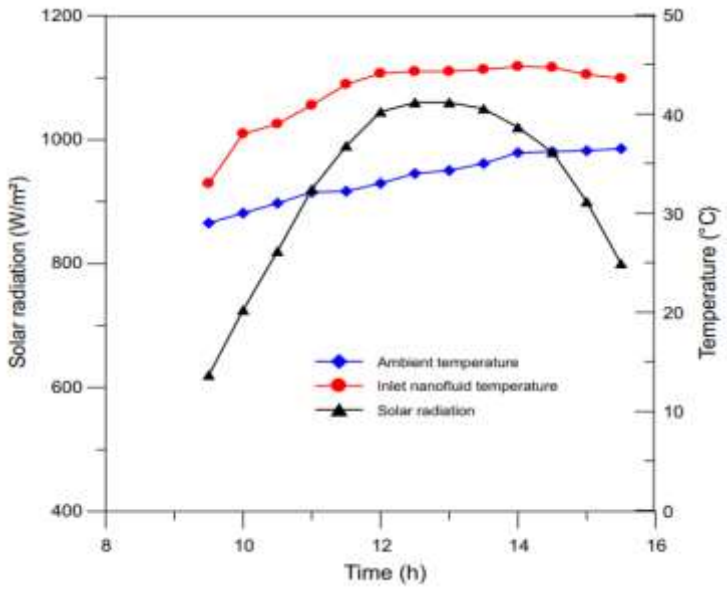

Figure 9: The reference graph of change in temperature and the radiation intensity with change in time

3.7 Calculations

All the calculations are done on the steady state conditions where the plate and absorber plate and the insulation all are on their respective steady state condition and none of them have variation in temperature in x or y –axis.

Internal Energy Change of Absorber Plate:

$$\Delta U_{pab} = 730.12(T_{pv} - T_{pab}) + 7031.6(T_{tu} - T_{pv}) + 0.8125(T_i - T_{pab})$$

Internal Energy Change of Tube:

$$\Delta U_t = = 7031.6(T_{pv} - T_{tu}) + 319.30(T_f - T_{tu})$$

Internal Energy Change of Fluid in Tube:

$$\Delta U_{nf} = 7031.6(T_t - T_{nf}) - \dot{m}C_{nf}\Delta T_{nf}$$

3.8 Heating Element

Since we are developing a hybrid heating system, it will heat water on both, the heat input from the plates and the heating element powered by PV plates output. Our heating element is Magnesium Oxide and Nichrome-based heating element with

stainless steel alloy casing. It works on 24V DC and consume 80 Watts. It is fitted in water storage tank and heat the water according to desired level.

Figure 10: DC Heating Element

3.9 Pump

We use Domiro DM-4000 diaphragm pump for circulating water in the tubes. It can handle a maximum pressure of 125 psi. It works on 12V DC and consume 5.5 Amps on maximum working conditions. It has a maximum flowrate of 5.5 Liters/Minute. We controlled is flowrate by using it with L298N motor Driver. L298N takes PWM input signal from Arduino and control its flow rate by varying the input voltage of pump.

Figure 11: Diaphragm Pump

3.10 Automated Control:

3.10.1 Microcontroller:

Arduino Mega is the brain of the control system. This micro-controller is used due to many reasons, mainly due to the ease of access and coding. It is easy to interface, comes with a built-in ADC and has an IDE with a bunch of libraries designed for control applications.

Figure 12: Arduino Mega 2560

Table 5: Specifications for the designated Arduino

Microcontroller	Arduino Mega 2560
Operating Voltage	5V
Input Voltage (recommended)	7 – 12V
Input Voltage (limits)	6 – 20V
Digital I/O Pins	54 (15 provide PWM output)
Analog Input Pins	16
DC Current per I/O Pin	20mA
DC Current for 3.3V Pin	50mA
Flash Memory	256KB of which 8KB is for bootloader
Clock Speed	16 MHz
Length	101.52mm
Width	53.3mm
Weight	37g

3.10.2 Temperature Sensor:

K-Type Thermocouple with MAX6675 amplifier is used to sense temperature of water and plates in our project. It is made out of Chromel and Alumel conductors. The MAX6675 digitizes the signal from the thermocouple. The output is given in a 12-bit resolution and it is SPI-compatible and read-only format. It resolves the temperatures to 0.25°C. It allows readings from 0°C to +1024°C, and give accuracy of 8 LSBs for temperatures range of 0°C to +700°C.

Figure 13: K-Type Thermocouple with MAX6675 Module

3.10.3 L298N Motor Driver:

The pump is connected to the micro-controller through the L298N motor Driver This is because Arduino cannot provide the required current to run the pump. The motor controller can provide us with a maximum supply voltage of around 50V.

For the control circuit, the terminals of the pump are connected with the OUT1 and OUT2 terminals of the L298N board. The flowrate of the pump can be controlled by using the bottom row of pins on the motor controller board. IN1 and IN2 terminals are used to control the motors connected at the OUT1 and OUT2 terminals, respectively. The motor controller takes input from the output of voltage regulator circuit that regulate a constant voltage supply of 12V provided by PV plates. It can also be powered by a 12V DC power supply. The PWM pins of the Arduino are used to control the flowrate of the pump using the EN pins.

Figure 14: L298N Motor Driver

Table 6: Specification Table of L298N Motor Controller

Driver Model	L298N
Driver Chip Driver	H Bridge L298N
Motor Supply Voltage (Maximum)	46V
Motor Supply Current (Maximum)	2A
Logic Voltage	5V
Driver Voltage	5 – 35V
Driver Current	2A
Logical Current	0 – 36mA
Maximum Power (W)	25W

3.10.4 Control Flow Chart:

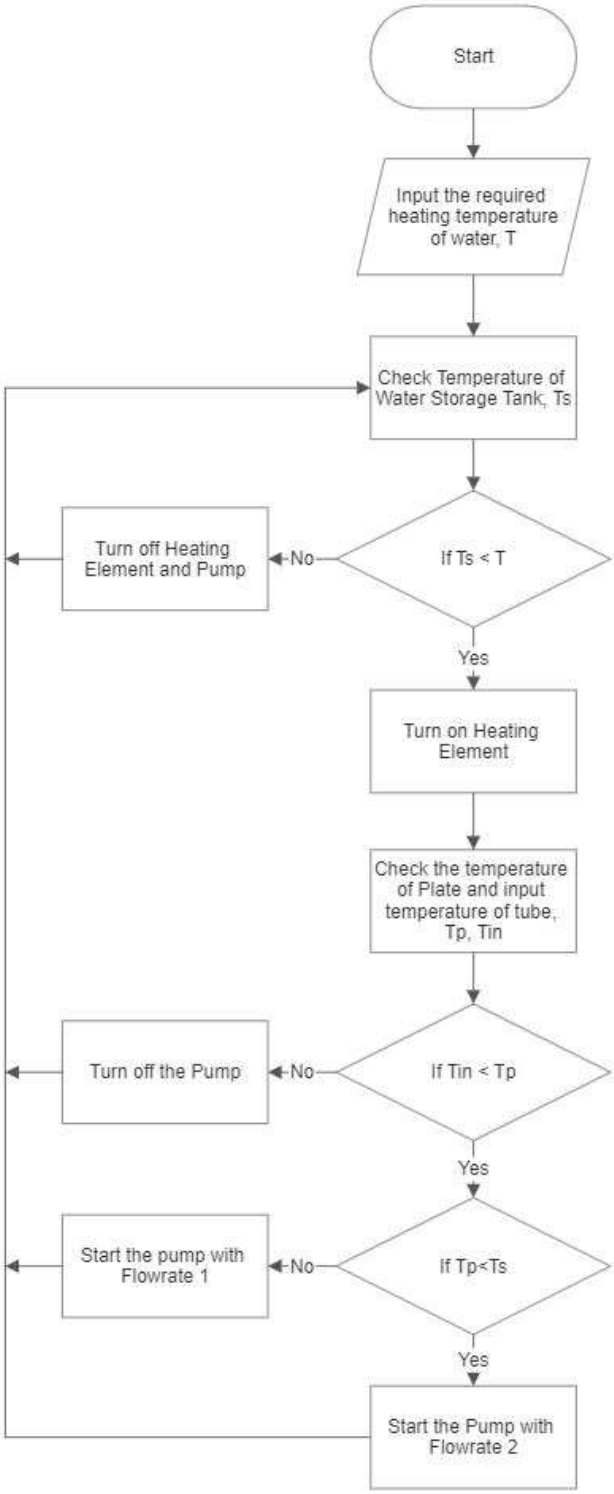

Figure 15: Control Flow Chart

3.10.5 Circuit Diagram:

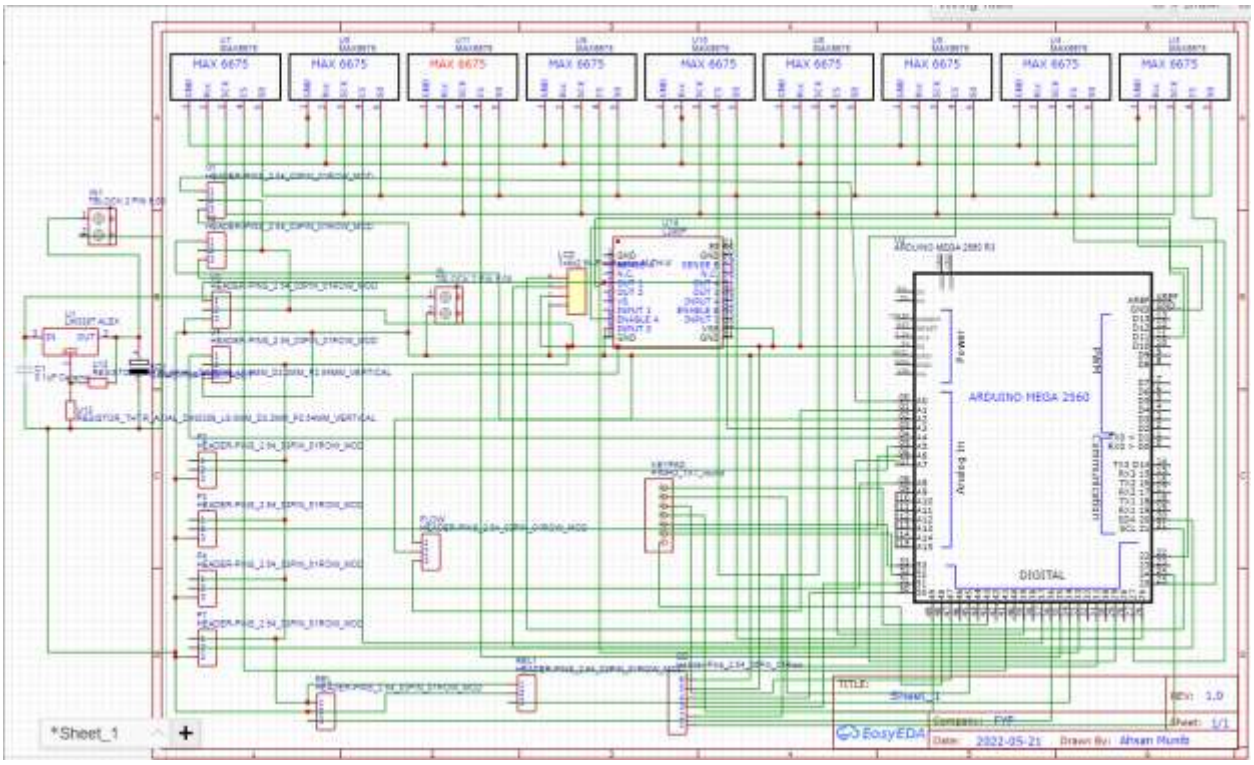

Figure 16: Circuit Diagram of Control Circuit

3.10.6 Code:

```
#include <Wire.h> // Library for I2C communication
#include <LiquidCrystal_I2C.h> // Library for LCD
#include "max6675.h" // Library for thermistor
#include <SPI.h> //Library for SPI communication (Pre-Loaded into Arduino)
#include <SD.h> //Library for SD card (Pre-Loaded into Arduino)
#include <Keypad.h>


// Wiring: SDA pin is connected to A4 and SCL pin to A5.
// Connect to LCD via I2C, default address 0x27 (A0-A2 not jumpered)
LiquidCrystal_I2C lcd = LiquidCrystal_I2C(0x27, 20, 4); // Change to
(0x27,20,4) for 20x4 LCD.


const int ROW_NUM = 4; //four rows
const int COLUMN_NUM = 4; //three columns

char keys[ROW_NUM][COLUMN_NUM] =
{
  {'1', '2', '3', 'A'},
  {'4', '5', '6', 'B'},
  {'7', '8', '9', 'C'},
```

```
  {'*', '0', '#', 'D'}
};

byte pin_rows[ROW_NUM] = {31, 33, 35, 37}; //connect to the row pinouts of
the keypad
byte pin_column[COLUMN_NUM] = {39, 41, 43, 45}; //connect to the column
pinouts of the keypad

Keypad keypad = Keypad( makeKeymap(keys), pin_rows, pin_column, ROW_NUM,
COLUMN_NUM );
String inputString;
long inputInt;


const int chipSelect = 24; //SD card CS pin connected to pin 4 of Arduino
int num = 0;


int count = 0;


// Motor connections
int enA = 11;
int in1 = 22;
int speedPWM = 0;


const int voltageSensor = A1;
const int voltageSensor1 = A2;

float vOUT = 0.0;
float vIN = 0.0;
float R1 = 30000.0;
float R2 = 7500.0;
int value = 0;


int soPin = 26;// SO=Serial Out -Common for all five sensors
int csPin1 = 47;// CS = chip select CS pin
int csPin2 =  49;
int csPin3 =  38;
int csPin4 =  53;
int csPin5 =  40;
//int csPin6 = 35;
//int csPin7 = 37;
//int csPin8 = 39;
//int csPin9 = 41;
int sckPin = 52;// SCK = Serial Clock pin -Commonm for all five sensors
MAX6675 Module1(sckPin, csPin1, soPin);// create instance object of MAX6675
MAX6675 Module2(sckPin, csPin2, soPin);
MAX6675 Module3(sckPin, csPin3, soPin);
MAX6675 Module4(sckPin, csPin4, soPin);
MAX6675 Module5(sckPin, csPin5, soPin);

int heat = 36; //relay pin controlling heating element
```

```
int temp = 0;

int X;
int Y;
float TIME = 0;
float FREQUENCY = 0;
float WATER = 0;
float TOTAL = 0;
float LS = 0;
const int reading = A1;


float temperature1 = 0;
float temperature2 = 0;
float temperature3 = 0;
float temperature4 = 0;
float temperature5 = 0;


int lastState = HIGH; // the previous state from the input pin
int currentState;

char key;


void Write_SDcard()
{
  // open the file. note that only one file can be open at a time, so you
have to close this one before opening another.
  File dataFile = SD.open("LoggerCD.txt", FILE_WRITE);

  // if the file is available, write to it:
  if (dataFile)
  {
    dataFile.print(num); //Store date on SD card
    dataFile.print(" - "); //Move to next column using a ","

    dataFile.print(temperature1); //Store date on SD card
    dataFile.print(" - "); //Move to next column using a ","

    dataFile.print(temperature2); //Store date on SD card
    dataFile.print(" - "); //Move to next column using a ","

    dataFile.print(temperature3); //Store date on SD card
    dataFile.print(" - "); //Move to next column using a ","

    dataFile.print(temperature4); //Store date on SD card
    dataFile.print(" - "); //Move to next column using a ","

    dataFile.print(temperature5); //Store date on SD card
    dataFile.print(" - "); //Move to next column using a ","

    dataFile.print(WATER); //Store date on SD card

    dataFile.println(); //End of Row move to next row
```

```
    dataFile.close(); //Close the file
  }
  else
  {
    Serial.println("OOPS!! SD card writing failed");
  }
}


void Initialize_SDcard()
{
  // see if the card is present and can be initialized:
  if (!SD.begin(chipSelect))
  {
    Serial.println("Card failed, or not present");
    // don't do anything more:
    return;
  }
  // open the file. note that only one file can be open at a time, so you
have to close this one before opening another.

  File dataFile = SD.open("LoggerCD.txt", FILE_WRITE);

  // if the file is available, write to it:
  if (dataFile)
  {
    dataFile.println("Reading - Temperature1 - Temperature2 - Temperature3 -
Temperature4 - Temperature5 - Flowrate"); //Write the first row of the excel
file

    dataFile.close();
  }
}

const int currentPin = A15;
int sensitivity = 66;
int adcValue= 0;
int offsetVoltage = 2500;
double adcVoltage = 0;
double currentValue = 0;

const int currentPin1 = A14;
int adcValue1= 0;
int offsetVoltage1 = 2500;
double adcVoltage1 = 0;
double currentValue1 = 0;


void setup()
{
  Serial.begin(9600);
  // Set all the pump pins to outputs
  pinMode(enA, OUTPUT);
  pinMode(in1, OUTPUT);
  pinMode(heat, OUTPUT);
  pinMode(reading, INPUT);
```

```
  pinMode(voltageSensor, INPUT);
  pinMode(voltageSensor1, INPUT);



  // Turn off pump - Initial state
  digitalWrite(in1, LOW);
  // Initiate the LCD:
  lcd.init();
  lcd.backlight();


  inputString.reserve(3); // maximum number of digit for a number is 3,
change if needed


  Initialize_SDcard();


  lcd.setCursor(0, 0); // Set the cursor on the first column and first row.
  lcd.print("WELCOME"); // Print the string "Hello World!"
  delay(5000);
  lcd.clear();
  lcd.setCursor(0, 0); //Set the cursor on the third column and the second
row (counting starts at 0!).
  lcd.print("Enter the max temp:");
  lcd.setCursor(0, 1);
  delay(3500);
  if (key >= '0' && key <= '9')
  { // only act on numeric keys
    inputString += key;               // append new character to input string
  }
  else if (key == '#')
  {
    if (inputString.length() > 0)
    {
      inputInt = inputString.toInt(); // YOU GOT AN INTEGER NUMBER
      inputString = "";               // clear input
      temp = inputInt;// DO YOUR WORK HERE
    }
  }
  delay(3500);
  lcd.clear();
  lcd.setCursor(0, 0);
  lcd.print("Enter PWM value:");
  lcd.setCursor(0, 1);
  delay(4000);
  while (key != keypad.getKey())
  {}
  if (key >= '0' && key <= '9')
  { // only act on numeric keys
    inputString += key;               // append new character to input string
  }
  else if (key == '#')
  {
    if (inputString.length() > 0)
```

```
    {
      inputInt = inputString.toInt(); // YOU GOT AN INTEGER NUMBER
      inputString = "";               // clear input
      speedPWM = inputInt;// DO YOUR WORK HERE
    }
  }
  lcd.clear();
}

void loop()
{


  value = analogRead(voltageSensor);
  vOUT = (value * 5.0) / 1024.0;
  vIN = vOUT / (R2 / (R1 + R2));

  int value1 = analogRead(voltageSensor1);
  int vOUT1 = (value1 * 5.0) / 1024.0;
  float vIN1 = vOUT1 / (R2 / (R1 + R2));

  adcValue = analogRead(currentPin);
  adcVoltage = (adcValue / 1024.0) * 5000;
  currentValue = ((adcVoltage - offsetVoltage) / sensitivity);

  adcValue1 = analogRead(currentPin1);
  adcVoltage1 = (adcValue1 / 1024.0) * 5000;
  currentValue1 = ((adcVoltage1 - offsetVoltage1) / sensitivity);

  digitalWrite(in1, HIGH);
  analogWrite(enA, speedPWM);
  temperature2 = Module2.readCelsius();
  if (temperature2 > temp)
  {
    digitalWrite(heat, HIGH);
  }
  else
  {
    digitalWrite(heat, LOW);


    // basic readout test, just print the current temp
    temperature1 = Module1.readCelsius();
    if (temperature1 > 45)
    {
      // Turn on motors
      digitalWrite(in1, HIGH);

//      speedPWM = map(temperature1, 45, temp, 100, 255); // variable, from
low, from high, to low, to high
//      analogWrite(enA, speedPWM);
    }

    temperature1 = Module1.readCelsius();
    Serial.print("C1 = ");
    Serial.println(temperature1);
```

```
temperature2 = Module2.readCelsius();
Serial.print("C2 = ");
Serial.println(temperature2);

temperature3 = Module3.readCelsius();
Serial.print("C3 = ");
Serial.println(temperature3);

temperature4 = Module4.readCelsius();
Serial.print("C4 = ");
Serial.println(temperature4);

temperature5 = Module5.readCelsius();
Serial.print("C5 = ");
Serial.println(temperature5);

X = pulseIn(reading, HIGH);
Y = pulseIn(reading, LOW);
TIME = X + Y;
FREQUENCY = 1000000 / TIME;
WATER = FREQUENCY / 7.5;
LS = WATER / 60;
delay(1000);

lcd.clear();
lcd.setCursor(0, 0);
lcd.print("Flowrate:");
lcd.setCursor(11, 0);
lcd.print(WATER);
lcd.setCursor(0, 2);
lcd.print("Voltage:");
lcd.setCursor(9, 2);
lcd.print(vIN);
lcd.setCursor(0, 3);
lcd.print("Voltage:");
lcd.setCursor(9, 3);
lcd.print(vIN1);
delay(5000);
lcd.clear();
lcd.setCursor(0, 0);
lcd.print("Current:");
lcd.setCursor(11, 0);
lcd.print(currentValue);
lcd.setCursor(0, 2);
lcd.print("Current:");
lcd.setCursor(9, 2);
lcd.print(currentValue1);
delay(5000);
lcd.clear();

lcd.setCursor(0, 0);
lcd.print("Temp 1:");
lcd.setCursor(8, 0);
lcd.print(temperature1);
lcd.setCursor(0, 1);
```

```
    lcd.print("Temp 2:");
    lcd.setCursor(8, 1);
    lcd.print(temperature2);
    lcd.setCursor(0, 2);
    lcd.print("Temp 3:");
    lcd.setCursor(8, 2);
    lcd.print(temperature3);
    lcd.setCursor(0, 3);
    lcd.print("Temp 4:");
    lcd.setCursor(8, 3);
    lcd.print(temperature4);
    delay(1500);
    lcd.clear();
    lcd.setCursor(0, 0);
    lcd.print("Temp 5:");
    lcd.setCursor(8, 0);
    lcd.print(temperature5);

    if (count == 5)
    {
      Write_SDcard();
      count = 0;
    }
  }

  num++;
  count++;

}
```

3.11 Schematic Diagram of Project

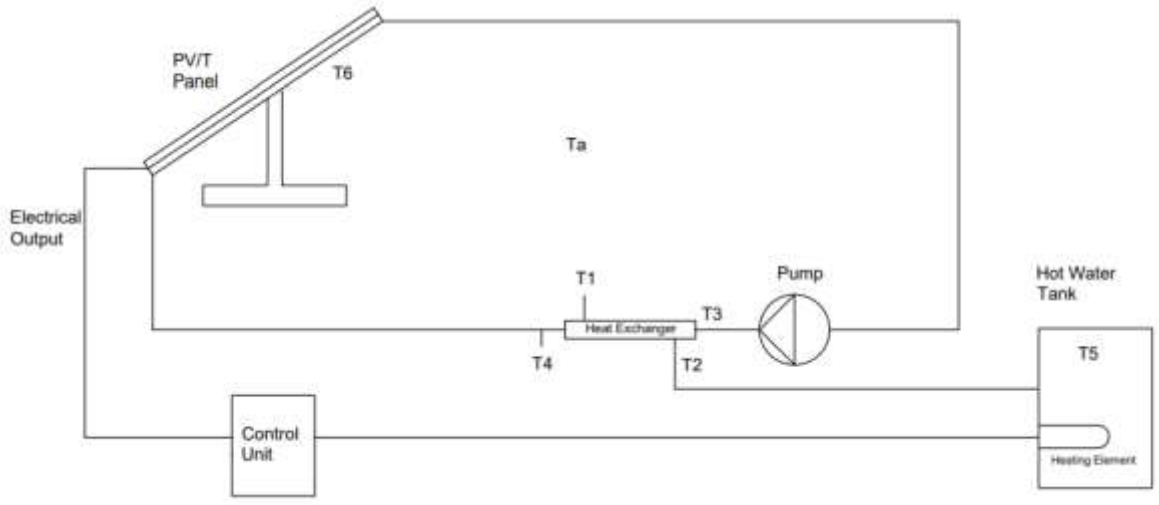

Figure 17: Schematic Diagram of Project

3.12 General Setting of Equipment

Figure 18: General Setting of equipment

CHAPTER 4: RESULTS AND DISSCUSSIONS

4.1 The thermal and electrical efficiency of the system without insulation

Thermal efficiency

1. As **ṁ is 0.07kg/s**, C_p is 4186J/kg.K, A_c is 0.011886m^2 , G is 900W/m^2 and Change in temperature is 2K.

$$\eta_{th} = \dot{m}C_{p,nf}(T_{out} - T_{in}) / A_cG$$

$$\eta_{th} = 0.07 \times 4186 \times 2 / (0.011 \times 900)$$

$$\eta_{th} = 59.19\%$$

Electrical efficiency

It deduces 2 degrees per cycle which makes reduction to the temperature of plate to 1 degree and the cycle continues till the temperature difference of fluid and plate become 5degrees Celsius.

Before cooling

$$\eta_{elec} = \eta_0[1 - \beta (T_{pv} - 298)] \qquad \text{as } T_{pv} \text{ is } 50^oC$$

$$\eta_{elec} = 13.5\%$$

After Cooling

$$\eta_{elec} = \eta_0[1 - \beta (T_{pv} - 298)] \qquad \text{as } T_{pv} \text{ is } 40^oC$$

$$\eta_{elec} = 14.1\%$$

Thermal efficiency

2. As **ṁ is 0.03kg/s**, C_p is 4186J/kg.K, A_c is 0.011886m^2 , G is 900W/m^2 and Change in temperature is 3.5K.

$$\eta_{th} = \dot{m}C_{p,nf}(T_{out} - T_{in}) / A_cG$$

$$\eta_{th} = 0.03 \times 4186 \times 3.5 / (0.011 \times 900)$$

$$\eta_{th} = 40.7\%$$

Electrical efficiency

It deduces 3.5 degrees per cycle which makes reduction to the temperature of plate to 2 degree and the cycle continues till the temperature difference of fluid and plate become 5degrees Celsius.

Before cooling

$$\eta_{elec} = \eta_0[1 - \beta (T_{pv} - 298)] \qquad \text{as } T_{pv} \text{ is } 50^oC$$

$$\eta_{elec} = 13.5\%$$

After Cooling

$$\eta_{elec} = \eta_0[1 - \beta (T_{pv} - 298)] \qquad \text{as } T_{pv} \text{ is } 35^oC$$

$$\eta_{elec} = 14.4\%$$

As β and η_0 are 0.4% and 15% respectively.

So, we can see the change in efficiency of the project change by the change in the flow rate condition and as well as the temperature difference also increases with the deficiency in flow rate. And also affects the electrical efficiency as if the flow rate is slow more heat can be extracted from the plate and electrical efficiency increases but at the negligible energy benefit is seemed.

4.2 The thermal efficiency of the system with insulation

$$\eta_{th} = \dot{m}C_{p,nf}(T_{out} - T_{in}) / A_cG$$

Thermal efficiency

1. As $\dot{m}$ is 0.07kg/s, C_p is 4186J/kg.K, A_c is 0.011886m^2 , G is 900W/m^2 and Change in temperature is 3K.

$$\eta_{th} = \dot{m}C_{p,nf}(T_{out} - T_{in}) / A_c G$$

$$\eta_{th} = 0.07 \times 4186 \times 3 / (0.011 \times 900)$$

$$\eta_{th} = 82.17\%$$

Electrical efficiency

It deduces 3 degrees per cycle which makes reduction to the temperature of plate to 0.5 degree just because of the heat accumulated due to the insulation applied and the cycle continues till the temperature difference of fluid and plate become 5degrees Celsius.

Before cooling

$$\eta_{elec} = \eta_0[1 - \beta (T_{pv} - 298)] \qquad \text{as } T_{pv} \text{ is } 50^oC$$

$$\eta_{elec} = 13.5\%$$

After Cooling

$$\eta_{elec} = \eta_0[1 - \beta (T_{pv} - 298)] \qquad \text{as } T_{pv} \text{ is } 45^oC$$

$$\eta_{elec} = 13.8\%$$

As β and η_0 are 0.4% and 15% respectively.

Thermal efficiency

2. As $\dot{m}$ is 0.03kg/s, C_p is 4186J/kg.K, A_c is 0.011886m^2 , G is 900W/m^2 and Change in temperature is 5K.

$$\eta_{th} = \dot{m}C_{p,nf}(T_{out} - T_{in}) / A_c G$$

$$\eta_{th} = 0.03 \times 4186 \times 5 / (0.011 \times 900)$$

$$\eta_{th} = 58\%$$

Electrical efficiency

It deduces 5 degrees per cycle which makes reduction to the temperature of plate to 1 degree just because of the heat accumulated due to the insulation applied and the cycle continues till the temperature difference of fluid and plate become 5degrees Celsius.

Before cooling

$$\eta_{elec} = \eta_0[1 - \beta\,(T_{pv} - 298)] \qquad \text{as } T_{pv} \text{ is } 50^oC$$

$$\eta_{elec} = 13.5\%$$

After Cooling

$$\eta_{elec} = \eta_0[1 - \beta\,(T_{pv} - 298)] \qquad \text{as } T_{pv} \text{ is } 40^oC$$

$$\eta_{elec} = 14.1\%$$

As β and η_0 are 0.4% and 15% respectively.

Table 7: Efficiency change without insulation with change in flow rate)

Mass Flow Rate (kg/s)	Thermal efficiency	Electrical efficiency Before Cool	Electrical efficiency After Cool
0.03	57.1	13.5	14.8
0.05	52.9	13.5	14.7
0.07	44.4	13.5	14.5
0.08	33.83	13.5	14.3

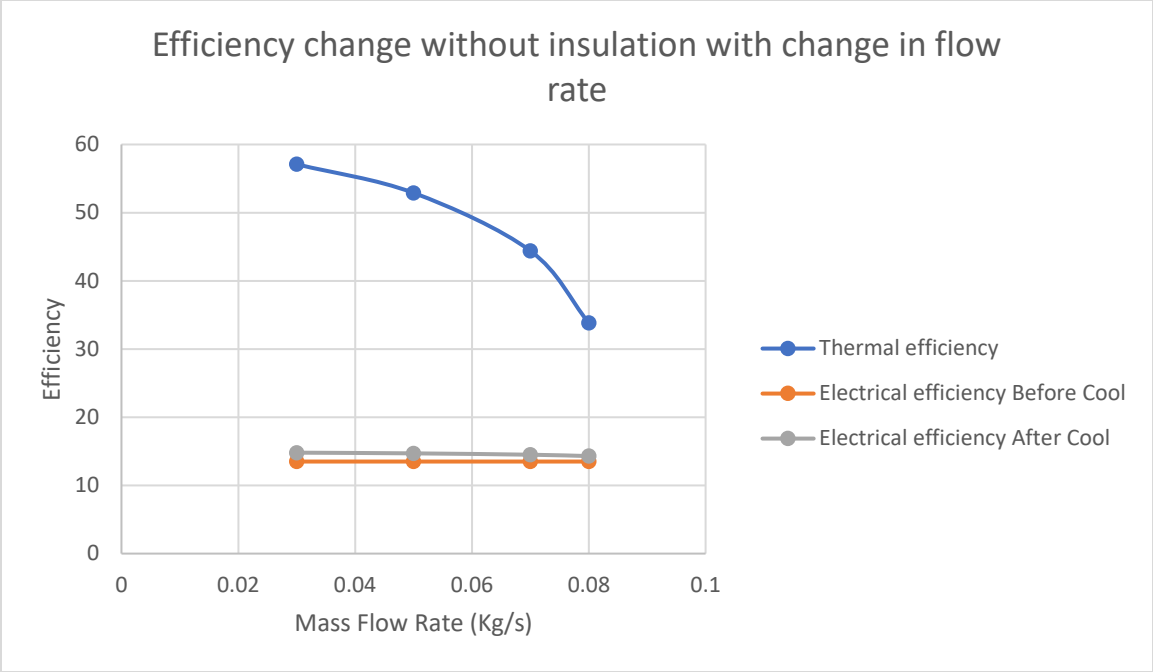

Figure 19: Efficiency change without insulation with change in flow rate

Table 8: Efficiency change with insulation with change in flow rate

Mass Flow Rate (kg/s)	Thermal efficiency	Electrical efficiency Before Cool	Electrical efficiency After Cool
0.03	62.7	13.5	14.6
0.05	57.5	13.5	14.5
0.07	48.3	13.5	14.3
0.08	39.4	13.5	14.1

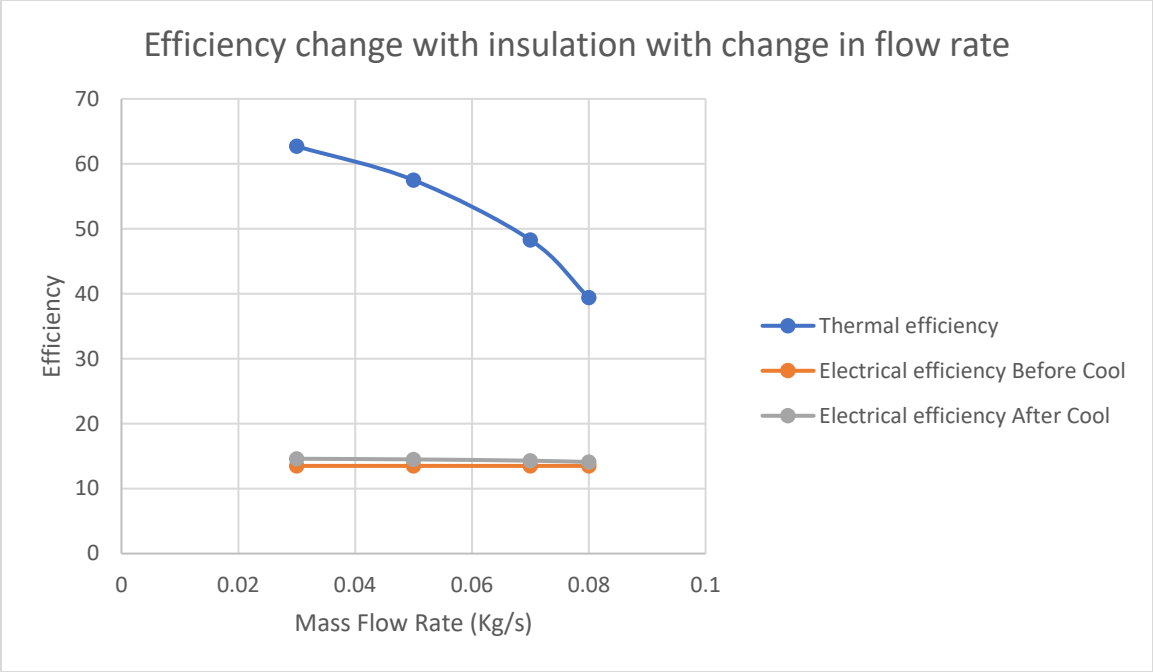

Figure 20: Efficiency change with insulation with change in flow rate

So, we can see the change in efficiency of the project by the change in the flow rate condition and as well as the temperature difference also increases with the deficiency in flow rate. Also, the thermal efficiency increases with the applying of the insulation just because of the temperature change increases in the tubes as the insulation don't allow heat to go out so the efficiency increases. And also affects the electrical efficiency as if the flow rate is slow more heat can be extracted from the plate and electrical efficiency increases but at the negligible energy benefit is seemed. But it became less due to insulation applied.

CHAPTER 5: CONCLUSIONS AND RECCOMENDATIONS

5.1 Conclusion

The conclusion of the results we gained in the experiment we take in this project are that

- We get approximately 50^{o}C at 11am to 3pm only by the heat exchanger.
- The thermal efficiency gained is accountable and we can see the difference in the temperature between inlet and outlet temperature.
- Approximately the 50% of thermal efficiency can be achieved by the panel especially by applying the insulation.

The results gained by the experiment are our results we get from the experimentation and also the efficiency is approximately 60 percent and the temperature gained in the storage tank is approximately 50^{o} at 11am to 3pm and the remaining temperature can be achieved by the heating element in the storage tank.

5.2 Future Recommendations

- This study can be extended in future with using nano-Fluids as a transport fluid in hybrid heating system.
- Efficiency of PV plates can be further enhanced by developing an automated dust cleaning system.
- For better automated control, we can use PID control algorithm to achieve accurate temperature control.

REFERENCES

[1] Khan, M.A.; Khan, J.A.; Ali, Z.; Ahmad, I.; Ahmad, M.N. The challenge of climate change and policy response in Pakistan. Environmental Earth Sciences 2016, 75, 412.

[2] Farooqi, A.B.; Khan, A.H.; Mir, H.J.P.J.o.M. Climate change perspective in Pakistan. 2005, 2.

[3] Tiwari A, Barnwal P, Sandhu GS, Sodha MS. Energy metrics analysis of hybrid—photovoltaic (PV) modules. Appl Energy 2009;86:2615–25.

[4] Tyagi VV, Kaushik SC, Tyagi SK. Advancement in solar photovoltaic thermal (PVT) hybrid collector technology. Renewable Sustainable Energy Rev 2012;16:1383–98.

[5] Zondag H, Bakker M, Van Helden W. 2006. PVT roadmap/An European guide for the development and market production of PV–thermal technology. In: PV Catapult—contract no. 502775 (SES6). Energy Research Centre of the Netherlands ECN2006.

[6] Chapin DM, Fuller CS, Pearson GL. A new silicon p–n junction photocell for converting solar radiation into electrical power. J Appl Phys 1954;25:676–7.

[7] Eckstein, David & Künzel, Vera & Schäfer, Laura. (2021). GLOBAL CLIMATE RISK INDEX 2021.

[8] Climate Risk Country Profile: Pakistan (2021): The World Bank Group and the Asian Development Bank.

[9] J. F. Geisz et al., "Building a Six-Junction Inverted Metamorphic Concentrator Solar Cell," in IEEE Journal of Photovoltaics, vol. 8, no. 2, pp. 626-632, March 2018.

[10] M. A. Green, E. D. Dunlop, D. H. Levi, J. Hohl-Ebinger, M. Yoshita, and A. W. Ho-Baillie, “Solar cell efficiency tables (version 54),” Prog. Photovoltaics 27, 565–575 (2019).

[11] K. Yoshikawa, H. Kawasaki, W. Yoshida, T. Irie, K. Konishi, K. Nakano, T. Uto, D. Adachi, M. Kanematsu, H. Uzu et al., “Silicon heterojunction solar cell with interdigitated back contacts for a photoconversion efficiency over 26%,” Nat. Energy 2, 17032 (2017).

[12] Grubišić-Čabo, F, Nižetić, S, Marinić Kragić, I, Čoko, D. Further progress in the research of fin-based passive cooling technique for the free-standing silicon photovoltaic panels. Int J Energy Res. 2019; 43: 3475– 3495.

[13] M. S. Abd-Elhady, Z. Serag, and H. A. Kandil, “An innovative solution to the over-heating problem of PV panels,” Energy Convers. Manage. 157, 452–459 (2018).

[14] Y. Wang, Y. Gao, Q. Huang, G. Hu, and L. Zhou, “Experimental study of active phase change cooling technique based on porous media for photovoltaic thermal management and efficiency enhancement,” Energy Convers. Manage. 199, 111990 (2019).

[15] Y. M. Irwan, W. Z. Leow, M. Irwanto, M. Fareq, S. I. S. Hassan, I. Safwati, and A. R. Amelia, “Comparison of solar panel cooling system by using DC brushless fan and DC water,” J. Phys. 622, 12001 (2015).

[16] A. Shukla, K. Kant, A. Sharma, and P. H. Biwole, “Cooling methodologies of photovoltaic module for enhancing electrical efficiency: A review,” Sol. Energy Mater. Sol. Cells 160, 275–286 (2017).

[17] Zondag, H.A. Flat-plate PV-Thermal collectors and systems: A review. Renewable and Sustainable Energy Reviews 2008, 12, 891-959.

[18] Buonomano, A.; Calise, F.; Vicidomini, M. Design, Simulation and Experimental Investigation of a Solar System Based on PV Panels and PVT Collectors. 2016, 9, 497.

[19] Chow, T.T. A review on photovoltaic/thermal hybrid solar technology. Applied Energy 2010, 87, 365-379.

[20] Kumar, A.; Baredar, P.; Qureshi, U. Historical and recent development of photovoltaic thermal (PVT) technologies. Renewable and Sustainable Energy Reviews 2015, 42, 1428-1436.

[21] Waqas, A.; Ud Din, Z. Phase change material (PCM) storage for free cooling of buildings—A review. Renewable and Sustainable Energy Reviews 2013, 18, 607-625.

[22] Sayyah, A.; Horenstein, M.N.; Mazumder, M.K. Energy yield loss caused by dust deposition on photovoltaic panels. Solar Energy 2014, 107, 576-604.

[23] (Vanek and Albright, 2008)

[24] https://www.sciencedirect.com/science/article/pii/B9781782422693500048

[25] K.Y. Leong, R. Saidur, S.N. Kazi, A.H. Mamun, Appl. Thermal Eng. 30, "Performance investigation of an automotive car radiator operated with nanofluid-based coolants (nanofluid as a coolant in a radiator)", 2685- 92 (2010)

[26] A.M. Hussein, R.A. Bakar, K. Kadirgama, K. V. Sharma, Int. Comm. In Heat and Mass Transf. 53, "Heat transfer enhancement using nanofluids in an automotive cooling system", 195-202 (2014)

[27] D.G. Subhedar, B.M. Ramani, A. Gupta, Heat Transf. Asian Research 46, "Experimental Investigation of Overall Heat Transfer Coefficient of Al2O3/Water–Mono Ethylene Glycol Nanofluids in an Automotive Radiator"! 863-877 (2017).

[28] N. Bozorgan, K. Krishnakumar, N. Bozorgan, Modern Mech. Eng. 2, "Numerical Study on Application of CuO- Water Nanofluid in Automotive Diesel Engine Radiator", 130-136 (2012).

[29] I. Elbadawy, M. Elsebay, M. Shedid and M. Fatouh, Int. J. of Automotive Tech. 19, “Reliability of nanofluid concentration on the heat transfer augmentation in engine radiator”, 233-43 (2018).